Project no. 282688

ECLIPSE

Evaluating the **Cl**imate and Air Quality **Im**p**a**cts of **S**hort-Liv**e**d Pollutants

Collaborative Project

Work programme: Climate forcing of non UnFCCC gases, aerosols and black carbon
Activity code: ENV.2011.1.1.2-2
Coordinator: Andreas Stohl, NILU - Norsk institutt for luftforskning

Start date of project: November 1st, 2011
Duration: 36 months

Deliverable 3.4.
SLCF plumes in model and reality

Due date of deliverable: project month 30
Actual submission date: project month 39

Organisation name of lead contractor for this deliverable: NILU
Scientist responsible for this deliverable: Sabine Eckhardt

Revision 1

Project co-funded by the European Commission within the Seventh Framework Programme (2007-2013)		
Dissemination Level		
PU	Public	
PP	Restricted to other programme participants (including the Commission Services)	X
RE	Restricted to a group specified by the consortium (including the Commission Services)	
CO	Confidential, only for members of the consortium (including the Commission Services)	

Summary

The concentrations of sulfate, black carbon (BC) and other aerosols in the Arctic are characterized by relatively high values in late winter and spring (so-called Arctic Haze) and low values in summer. Models have long been struggling to capture this seasonality and especially to reproduce the high concentrations associated with the Arctic Haze. In this study, we evaluate sulfate and BC concentrations from eleven different models driven with the same emission inventory against a comprehensive pan-Arctic measurement data set over a time period of two years (2008-2009). The set of models consisted of one Lagrangian particle dispersion model, four chemistry-transport models (CTMs), one atmospheric chemistry-weather forecast model and five chemistry-climate models (CCMs), of which two were nudged to meteorological analyses and three were running freely. The measurement data set consisted of surface measurements of equivalent BC (eBC) from six stations (Alert, Barrow, Station Nord, Pallas, Tiksi and Zeppelin) and aircraft measurements of refractory BC (rBC) from six different campaigns. We find that the models generally captured the measured eBC/rBC and sulfate measurements quite well, compared to past comparisons. However, the aerosol seasonality at the surface is still too weak in most models. Concentrations of eBC and sulfate averaged over three (four for eBC) surface sites are underestimated in winter/spring in all but one model (model means for January-March underestimated by 57% and 41% for BC and sulfate, respectively), whereas concentrations in summer are overestimated in the model mean (by 60% and 33% for July-September), but with over- as well as underestimates present in individual models. The largest eBC underestimates, not included in the above multi-site average, are found for the station Tiksi, which is closest to potential source regions in Russia and where the annual mean eBC concentration is three times higher than the average annual mean for all other stations. This suggests an underestimate of BC sources in Russia in the emission inventory used, even though this inventory contains gas flaring as an important BC source there. Based on the campaign data, biomass burning was identified as another cause of the modelling problems, at least for spring 2008. For sulfate, very large differences were found in the model ensemble, with an apparent anti-correlation between modeled surface concentrations and total atmospheric columns. There is a strong correlation between observed sulfate and eBC with consistent sulfate/eBC slopes found for all Arctic stations, indicating that the sources contributing to sulfate and BC throughout the Arctic are similar and that the aerosols are internally mixed and undergo similar removal. However, only three models reproduced this finding, whereas sulfate and BC are weakly correlated in the other models. Overall, no class of models (e.g., CTMs, CCMs) performed better than the others and differences are largely due to the treatment of aerosol removal in the models.

Introductory Note: Deliverables 3.3 (UPMC) and 3.4 (NILU)

Work Package 3 in the ECLIPSE project deals with the evaluation of ECLIPSE models through the comparison with data over source and receptor regions. D3.1 summarizes the findings over 2 source regions: Europe and Asia whereas D3.2 provided a preliminary assessment of model performance over the Arctic, the main receptor region considered in the ECLIPSE project since it is a major receptor of mid-latitude pollution and a key region for Arctic and global climate change. Deliverables 3.3. (UPMC) and 3.4 (NILU) have common goals which encompass the evaluation of the long-range transport of short-lived climate forcers (SLCFs) from source regions to our chosen receptor region, the Arctic. In addition, the work presented in these 2 deliverable reports benefited from the considerable investment and participation of ECLIPSE scientists in a report being prepared by the Arctic Council AMAP Expert Group on Black Carbon and Ozone impacts on Climate in the Arctic of which several ECLIPSE scientists are members. As part of this report, which will be published in spring 2015, ECLIPSE/AMAP models have been evaluated against monthly surface data and sonde/aircraft vertical profile data in the Arctic. This participation in AMAP allowed us to extend the ECLIPSE model evaluations to include up to 11 models for aerosols and 6 models for trace gas species. It allowed us to evaluate model performance in terms of pollutant transport to the Arctic as well as chemical and aerosol processing. Models with substantially different representations of pollutant transport which can have a significant effect on the representation of various SLCF distributions, participated in this work.

D3.3 focuses on the long-range transport of SLCFs between source and receptor regions. Here, we primarily assess the ability of models to correctly simulate distributions of trace gases and aerosols in the Arctic region; We make use of the considerable amount of data that was collected during the International Polar Year as part of POLARCAT and associated projects as well as data collected at surface monitoring sites. We evaluate model performance by comparing model results with aircraft, satellite and surface data. In particular, we show that improvements in the representation of black carbon emissions from oil/gas flaring in Russia and domestic wood burning in Scandinavia led to improved model simulations of the modelled black carbon seasonal cycle which had been severely underestimated at sites like Ny Alesund on Svalbard (Stohl et al., 2013). CALIPSO aerosol data is also used to evaluate models over the

entire Arctic region during spring and summer 2008. Models are also evaluated using carbon monoxide data, which provides an insight into model transport and species containing odd-nitrogen such nitrogen oxide (NO) and peroxy acetyl nitrate (PAN) that are important for tropospheric ozone, one of the main SLCFs considered in ECLIPSE. We also illustrate model capabilities for one pollution event in summer 2008 when Asian/Siberian fire pollution was transported directly across the Arctic to Greenland. A paper is in preparation on assessment of ozone radiative forcing in the Arctic including results from the ECLIPSE/AMAP model evaluation of ozone and its precursors based on the work presented here (Berntsen et al., 2014, prep.). A further manuscript based on this work is also in preparation focusing on uncertainties in pollution transport to the Arctic and implications for the Arctic ozone budget (Arnold, Law, et al., 2014).

D3.4 focuses on model evaluation of pollutant transport at different altitudes over receptor regions. Again, the Arctic is considered as the main receptor region. From previous studies it is known that long range to the Arctic is very poorly represented in models. In the case of aerosols, this is due to uncertainties in transport and scavenging. A study on the lifetime of aerosols determined by this 2 processes has been published in ACP (Kristiansen et al., 2013). An atmospheric lifetime of 10 - 14 days, which lies above commonly used aerosol lifetimes, could be determined. We have a strong focus on Arctic aerosols and specifically on, black carbon and sulfate in D3.4. The models results have been compared to surface data as well as data from aircraft campaigns. For BC in Spitsbergen a study was performed to find the influence of local emissions on the BC measured at the station. (Eckhardt et al., 2013). For the campaign data, the dispersion of pollution plumes was predicted and then sampled by aircraft in the Arctic. This enables us to see the vertical structure of SLCFs and is used to evaluate model performance. A manuscript submitted to ACP (Marelle et al.) is describing a case study of European pollution transport to the Arctic, facilitating POLARCAT-spring 2008 data. For D3.4 a manuscript is in preparation for submission to Atmospheric Chemistry and Physics: Eckhardt S., et al Validation of modeled BC and sulfate in the Arctic atmosphere. Here we perform a detailed comparison between all ECLIPSE model and observations.

Contributing Authors:

S. Eckhardt[1], B. Quennehen[2*], D. Olivié[6], T. Berntsen[3], R. Cherian[4], W. Collins[7,8], J. H. Christensen, N. Daskalakis[5], M. Flanner[12], A. Herber, C. Heyes, Ø. Hodnebrog[3], M. Kanakidou, Z. Klimont[9], J. Langer, K.S. Law[2], A. Massling, S. Myriokefalitakis, I. E. Nielsen, J. Quaas[4], P. Quinn, J.-C. Raut[2], S. T. Rumbold[7,8], M. Schulz[6], R. Skeie[3], H. Skov, M. T. Lund[3], K. von Salzen[10], Rashed Mahmood[11] and A. Stohl[1]

[1]{NILU - Norwegian Institute for Air Research, Kjeller, Norway}

[2]{Sorbonne Universités, UPMC Univ. Paris 06 ; Université Versailles St-Quentin ; CNRS/INSU ; LATMOS-IPSL, UMR 8190, Paris, France}

[3]{Center for International Climate and Environmental Research – Oslo (CICERO), Oslo, Norway}

[4]{Institute for Meteorology, Universität Leipzig, Germany}

[5]{Environmental Chemical Processes Laboratory, Department of Chemistry, University of Crete, Heraklion, Crete, Greece}

[6]{Norwegian Meteorological Institute, Oslo, Norway}

[7]{Met Office Hadley Centre, Exeter, UK}

[8]{University of Reading, Reading, UK}

[9]{International Institute for Applied Systems Analysis (IIASA), Laxenburg, Austria}

[10]{Canadian Centre for Climate Modelling and Analysis, Environment Canada, Victoria, British Columbia, Canada}

[11]{School of Earth and Ocean Sciences, University of Victoria, Victoria, British Columbia, Canada}

[12]{Department of Atmospheric, Oceanic, and Space Sciences, University of Michigan, Ann Arbor, MI, USA}

[] {Institute of Chemical Engineering Sciences (ICE-HT), Forth, Patra, Greece}

* - now at Univ. Grenoble Alpes/CNRS, Laboratoire de Glaciologie et Géophysique de l'Environnement (LGGE), 38041 Grenoble, France

1 Introduction

In addition to greenhouse gases, aerosols are important climate forcers (Ramanathan and Carmichael 2008; Myhre et al., 2013), but the magnitude of their forcing strongly depends on altitude, position relative to clouds, the surface albedo and the optical properties of the aerosol as well as cloud indirect effects, and it is highly uncertain. While absorbing aerosols such as black carbon (BC) are likely to increase climate warming (Shindell and Faluvegi, 2009), scattering aerosols such as sulfate have a cooling effect (Myhre et al., 2013). In addition to atmospheric radiative forcing, deposition of absorbing aerosols on snow or ice reduces the albedo and can thus induce faster melting and efficient surface warming (Jacobson, 2004; Flanner et al., 2009). The highly reflective surfaces of snow and ice as well as strong feedback processes make the Arctic a region of particular interest for aerosol research (Quinn et al., 2008).

The Arctic aerosol consists of a varying mixture of sulfate and organic carbon (OC), as well as ammonium, nitrate, BC and mineral dust (Quinn et al., 2007; Brock et al., 2011). Aerosols in the Arctic feature a strong annual cycle with a late winter/spring peak (the so-called "Arctic Haze") and a summer minimum. Increased transport during the cold season (Stohl, 2006) and increased removal by wet deposition during the warm season can explain this annual variation (Shaw, 1995; Law and Stohl, 2007) and also shape the aerosol size distribution (Tunved et al., 2013).

Models have for a long time struggled to capture the distribution of aerosols in the Arctic (Shindell et al., 2008; Koch et al., 2009). The concentrations of BC during the Arctic Haze season in particular were underestimated, partly by more than an order of magnitude (Shindell et al., 2008), whereas summer concentrations were sometimes overestimated. The simulated aerosol seasonality is strongly dependent on the model treatment of aerosol removal processes. For instance, changes in the calculation of aerosol microphysical properties, size distribution and removal can change simulated concentrations by more than an order of magnitude in remote regions such as the Arctic (Vignati et al., 2010) and the calculated Arctic BC mass concentrations are very sensitive to parameterizations of BC aging (conversion from hydrophobic to hydrophilic properties) and wet scavenging (Liu et al., 2011; Huang et al., 2010).

The seasonal decrease of aerosol concentrations from winter to summer in the Arctic is likely also due to the different efficiency of scavenging by different types of clouds. There is a transition from inefficient ice-phase cloud scavenging in winter to more efficient warm cloud scavenging in summer, and there is also the appearance of warm drizzling cloud in the late spring and summer boundary layer. Including these processes in a model clearly improved its performance both in terms of absolute concentrations as well as seasonality for sulfate and BC (Browse et al., 2012). This also seems to be in agreement with the observation-based findings that scavenging efficiencies are increased in summer both for light-scattering (of which sulfate is an important component) as well as for light-absorbing (of which BC is an important component) aerosols (Garrett et al., 2010, 2011). Another modeling problem may be excessive convective transport and underestimation of the associated wet scavenging in convective clouds, which can lead to model overestimates of BC in the upper troposphere and lower stratosphere (Allen and Landuyt, 2014; Wang et al., 2014). Despite remaining difficulties, the simulations of Arctic aerosols with many models have improved considerably in the last few years by updating the model treatment of some or all of the above mentioned processes (Fisher et al., 2011; Breider et al., 2014; Sharma et al., 2013; Lund and Berntsen, 2012; Allen and Landuyt, 2014).

Remaining problems may also be due to missing emission sources or incorrect spatial or temporal distribution of emissions in the inventories used for the modeling. The main sources of BC are biomass burning and incomplete combustion of fossil fuels and biofuels (Bond et al., 2004). Sulfate originates from natural sources such as oxidation of dimethyl sulphide (DMS) or sea salt over the oceans or volcanoes. It is also produced from oxidation of SO_2 emitted when sulphur-containing fossil fuels are burned or by metal smelting. Studies based on observed surface concentrations repeatedly suggest that the main source regions for Arctic BC and sulfate are located in high-latitude Eurasia (e.g., Sharma et al., 2006, Eleftheriadis 2009, Hirdman et al., 2010). Stohl et al. (2013) suggested that gas flaring in high-latitude Russia is an important source of BC which is missing from most inventories. In their simulations, BC emissions from gas flaring, coupled with enhanced domestic combustion in winter months, accounted for 42% of the annual mean BC surface concentrations in the Arctic and improved the simulation of Arctic BC concentrations compared to observations. However, they also noted the large uncertainty of the gas flaring emissions.

The radiative effects of aerosols are not so much determined by the surface concentrations but by the column loadings and they depend also on the altitude distribution of the aerosol (Samset et al., 2013; Samset and Myhre, 2011). Nevertheless, in the past, model results for the Arctic were evaluated mainly against surface measurements – even though they are not representative of the concentrations aloft, which are controlled partly by different source regions and different processes. It is therefore important to evaluate models not only against surface measurements but also using vertical profile information.

The purpose of this study is to explore the capabilities of a range of widely used chemistry transport models (CTMs) and chemistry climate models (CCMs) to simulate the Arctic aerosol concentrations. The models use a common emission inventory, which includes gas flaring emissions and provides monthly resolution of the emissions. Differences in modeled aerosol concentrations are therefore solely due to differences in the simulated transport, aerosol processing (e.g., sulphate formation, BC aging) and removal. We concentrate our investigations on BC and sulfate, for which we collected data from six surface stations and five aircraft campaigns in the Arctic.

2 Methods

2.1 Measurement data

Aerosol light absorption data were obtained from six sites in different parts of the Arctic: Alert, Canada (62.3°W, 82.5°N; 210 m above sea level (asl)), Station Nord, Greenland (16.67°W, 81.6°N; 30 m asl), Zeppelin/Ny Ålesund, Spitsbergen, Norway (11.9°E, 78.9°N; 478 m asl), Tiksi, Russia (128.9° E, 71.6°N; 1 m asl), Barrow, Alaska (156.6°W, 71.3°N; 11 m asl) and Pallas, Finland (24.12°E, 67.97°N; 565 m asl). The locations of these measurement stations are shown in Fig. 1. Different types of particle soot absorption photometers (PSAPs) were used for the measurements at Barrow, Alert, Station Nord and Zeppelin, a multi-angle absorption photometer was used at Pallas (Hyvärinen et al., 2011), and an aethalometer was used at Tiksi. All these instruments measure the particle light absorption coefficient σ_{ap}, each at its own specific wavelength (typically at around 530–550 nm), and for different size fractions of the aerosol (typically particles smaller than 1, 2.5 or 10 μm are sampled). Conversion of σ_{ap} to equivalent BC mass concentrations is not straightforward and requires certain assumptions. The mass absorption efficiency used for conversion is specific to the site, the instrument and the wavelength used and uncertain by at

least a factor of two. For Station Nord, a mass absorption efficiency of 3.9 $m^2 g^{-1}$ multiplied by a filter constant of 2 (i.e., a total of 7.8 $m^2 g^{-1}$) was used for conversion, based on comparison to elemental carbon measurements (Nguyen et al., 2013). For Tiksi, the conversion is done internally by the aethalometer. For the other sites, the measured light absorption was converted to BC mass concentration using a mass absorption efficiency of 10 $m^2 g^{-1}$, typical of aged BC aerosol (Bond and Bergstrom, 2006). Sharma et al. (2013) used the even higher value of 19 $m^2 g^{-1}$ for Barrow and Alert data. To reflect the uncertainties in this conversion, we refer to the converted light absorption values as equivalent BC (eBC).

For Barrow, Alert, Pallas, Zeppelin and Station Nord, eBC data were available for the years 2008-2009 and could be compared directly with model data which were available for the same period. At Tiksi, the measurements started only in 2009 and thus measured values for the period July 2009 to June 2010 were compared with modeled values for the year 2009. As the Tiksi data only became available very recently compared to data from the other stations, results were not provides for Tiksi from all models.

Barrow and Alert data are routinely subject to data cleaning, which shall remove the influence from local sources. Zeppelin generally is not strongly influenced by local emissions; however, summer values are enhanced by some 11% due to local cruise ship emissions (Eckhardt et al., 2013). The PSAP instrument at Station Nord was recently replaced by a multi-angle absorption photometer because of instrumental problems. However, for the period used here only the PSAP data were available. We use these data although its accuracy is not well known and its uncertainty is expected to be high.

Sulfate measurement data were available from the stations Pallas, Zeppelin, Barrow and Alert. The sulfate data were obtained on open face filters and cations and anions were subsequently quantified by ion chromatography. Non-sea salt (nss) sulfate concentrations were obtained by subtracting the sea salt contribution via analysis of Na^+ and Cl^- data, thus making the sulfate data directly comparable to the modeled nss-sulfate values. Samples were taken with daily to weekly resolution, depending on station and season.

Aircraft data were obtained from several campaigns. In the framework of POLARCAT (Polar Study using Aircraft, Remote Sensing, Surface Measurements, and Models of Climate Chemistry, Aerosols, and Transport), two ARCTAS (Arctic Research of the Composition of the Troposphere from Aircraft and Satellites) campaigns in April and June/July 2008 with a DC-8 aircraft covered mainly the North American Arctic (Jacob et al., 2010). The ARCPAC

(Aerosol, Radiation, and Cloud Processes affecting Arctic Climate; Brock et al., 2011) campaign was conducted from Alaska together with ARCTAS in April 2008. The PAMARCMiP (Polar Airborne Measurements and Arctic Regional Climate Model Simulation Project) campaign covered the entire western Arctic in April 2009 (Stone et al., 2010). Two HIPPO (High-Performance Instrumented Airborne Platform for Environmental Research Pole-to-Pole Observations; Schwarz et al., 2010; Schwarz et al., 2013; Wofsy et al., 2011) campaigns during January 2009 and October 2009 explored the North American Arctic. Flight legs north of 70°N for all of these campaigns are shown in Fig. 1. Refractory BC (rBC) was measured during these campaigns with single particle soot photometer (SP2) instruments (Kondo et al., 2001; Schwarz et al., 2006). Observations of submicrometer aerosol sulfate mass during ARCTAS were made with the PILS instrumentation package (Sullivan et al, 2006) using a mist chamber/ion chromatograh. Sulfate measurements during ARCPAC were made with a compact time-of-flight aerosol mass spectrometer (Bahreini et al., 2008).

During April 2008 agricultural and boreal influence was widespread throughout the Arctic (Warneke et al., 2010; Brock et al., 2011) and ARCTAS and ARCPAC partly targeted pollution plumes from these fires although Russian gas flaring may have also played a role. Anthropogenic pollution from Asia was also sampled by these campaigns in the western Arctic, particularly in the mid-upper troposphere (see Law et al., 2014 and refs therein). Pollution from Europe also made a significant contribution in the lower troposphere Europe. In contrast, PAMARCMiP and HIPPO sampled the Arctic atmosphere at times with little influence from biomass burning and also did not target pollution plumes. Thus, the higher mean rBC concentrations found during ARCTAS and ARCPAC than during PAMARCMiP a year later are caused both by the sampling strategy of these campaigns as well as the early start of the biomass burning season in 2008. Even though all available rBC and sulfate data from several campaigns were used for model evaluation, the data coverage and representativity for the Arctic as a whole must still be considered as rather poor. POLARCAT campaigns in the eastern arctic (e.g. POLARCAT-France) did not measure detailed chemical aerosol composition or were confined to the surface (e.g. ICEALOT ship campaign, Frossard et al., 2011).

ARCTAS-B was the only summertime POLARCAT campaign to make detailed measurements of BC and SO4 (Jacob et al., 2010). These flights focused mainly on boreal fires over Canada in July 2008 but with several flights into the high Arctic sampling, for

example Asian pollution close to the North Pole (Sodermann et al., 2010). Plume of Asian origin were also sampled in the upper troposphere over Canada (Singh et al., 2010).

2.2 Emissions

All models made use of an identical emission dataset, the ECLIPSE (Evaluating the Climate and Air Quality Impacts of Short-Lived Pollutants) emission inventory version V4a (Klimont et al., 2015a, 2015b). The ECLIPSE inventory was created using the GAINS (Greenhouse gas – Air pollution Interactions and Synergies) model (Amann et al., 2013), which provides emissions of long-lived greenhouse gases and shorter-lived species in a consistent framework. The proxies used in GAINS are consistent with those applied within the RCP (Representative Concentration Pathways) projections as described in Lamarque et al. (2010) and as further developed within the Global Energy Assessment project (GEA, 2012). They were, however, modified to accommodate for more recent information where available, e.g., on population distribution and open biomass burning, effectively making them year specific (Riahi et al., 2012; Klimont et al., 2013). For this study, emissions were provided for the years 2008 and 2009 and were lumped into the source categories industrial combustion, residential combustion, energy production, transport, agriculture, waste treatment, shipping, agricultural waste burning and gas flaring. All emission data were gridded consistently to a resolution of 0.5°x0.5°. Monthly disaggregation factors were provided for the domestic heating emissions, based on ambient air temperatures. For a more detailed description of the ECLIPSE emission data set, see Klimont et al. (2015a, 2015b). Non-agricultural biomass burning emissions were not available through GAINS and were therefore taken from the Global Fire Emission Database (GFED), version 3.1 (van der Werf et al., 2010). No attempt was made to harmonize sulfur emissions from volcanic sources or the ocean, which could explain some differences in simulated sulfate concentrations.

2.3 Models

We show results of 11 different models, whose main characteristics and references are summarized in Table 1. The horizontal resolution of the individual models ranges from about 0.6°x0.8° to 2.8°x2.8°. We use one Lagrangian particle transport model, FLEXPART (Flexible Particle Dispersion Model), which is run in backward mode for 30 days (thus, older source contributions are not accounted for). The simulation is driven by 1°x1° operational analyses from the European Centre for Medium Range Weather Forecast (ECMWF). The

OsloCTM2, TM4-ECPL (Tracer Model version 4 - Environmental Chemical Processes Laboratory) and SMHI MATCH (Swedish Meteorological and Hydrological Institute Multi-scale Atmospheric Transport and Chemistry Model) are CTMs and also use meteorological data from ECMWF. The DEHM (Danish Eulerian Hemispheric Model) CTM is driven by NCEP (National Centers for Environmental Prediction) meteorological data. WRF-Chem (Weather Research and Forecasting Model coupled with Chemistry) is an on-line atmospheric chemistry-weather forecast model which was nudged to NCEP FNL (final analysis) data for this study. The aerosol-climate model (ACM) ECHAM6-HAM2 (for brevity, referred to as ECHAM6 in figures) is the European Centre for Medium-Range Weather Forecasts Hamburg model version 6 (Stevens et al., 2013) extended with the Hamburg aerosol module version 2 (HAM2) (Zhang et al., 2012). ECHAM6-HAM2 and the CCMs HadGEM3 (Met Office Hadley Centre Climate Model, version 3) and CanAM4.2 (Canadian Atmospheric model, version 4.2) were nudged to ECMWF data. CESM1-CAM5.2 (Community Earth System Model version 1 – Community Atmosphere model version 5.2) and NorESM1-M (Norwegian Earth System Model version 1 with intermediate resolution, hereafter referred to as NorESM) are also CCMs but were running freely, thus producing their own meteorological data. These latter models cannot be compared point-to-point with the measurement data because they produced meteorological conditions which were different from the actual ones; however, longer-term (e.g., seasonal) means and variability should still be comparable with the measurements, especially since sea surface temperatures (SST) and sea-ice extent were prescribed and specific to the years 2008-2009. All models were sampled exactly at the locations of the measurement stations and along the flight tracks at the highest possible temporal resolution.

3. Simulated BC and sulfate concentrations

Figure 2 shows the simulated BC and sulfate column mass loadings as a function of latitude for the time periods of the Arctic Haze (March) and the much cleaner summer (July) in the Arctic, for the models for which this information was available. For BC in March, most models show a maximum near 20°N, with some models extending this maximum to 40°N. This covers approximately the latitude range with the highest global emissions where the models agree fairly well in their simulated column loadings. In contrast, large differences between the models are found in the Arctic, where column mass loadings vary by more than

an order of magnitude. Similar results are also found for sulfate, for which most models also show a maximum around 20-40°N; however, compared to BC, the models show a less pronounced decrease towards higher latitudes and two models even simulate increasing sulfate burdens with latitude. The relatively good agreement between the models in the BC and sulfate source region latitudes is not surprising, given that they all use the same emission data set. In contrast, the differences between the atmospheric column loadings in the Arctic must mainly be due to differences in the aerosol processing and removal and hence aerosol lifetimes, and probably differences in atmospheric transport. Most models with relatively low BC column loadings in the Arctic also have low sulfate loadings there, indicating correlation of the simulated removal of these two types of aerosols. A notable exception, however, is HadGEM3, which has moderately low BC but the highest sulfate loadings in the Arctic.

In July, the BC column loadings show a double peak in the southern tropics and northern subtropics. The southern tropical peak is due to the migration of the inter-tropical convergence zone (ITCZ) into the northern hemisphere, which leads to less efficient wet removal and dry conditions favoring biomass burning in the southern tropics. On the other hand, BC concentrations near 10°N show a deep minimum, due to the efficient wet removal near the ITCZ. Most models show a third peak in BC loading near 60°N, which results from open vegetation fires in the boreal region. North of 60°N, the BC loadings decline rapidly towards the North Pole. The sulfate column loading distribution in July lacks the peaks in the southern tropics and the boreal region because biomass burning is not a strong source of sulfate. HadGEM3 stands out against the other models even more than in spring, as its polar sulfate loadings are more than a factor five higher than those of all other models, which show a smooth decrease with latitude north of 40°N.

In the simulated surface BC and sulfate mass mixing ratios basically the same patterns are found as in the column loadings, but with enhanced gradients between source areas and remote regions (Fig. 3). When looking at individual models, there are, however, notable differences for sulfate. ECHAM6-HAM2 has the highest sulfate surface mass mixing ratios of all models, especially in the northern hemisphere subtropics and mid-latitudes. Combined with the rather “normal” column sulfate loadings of this model, this indicates that ECHAM6-HAM2 does not transport sulfate away from the surface as quickly as the other models. On the other hand, HadGEM3, which has by far the largest sulfate column loadings, has the smallest surface concentrations. This deficiency was due to the implementation of the Global

Model of Aerosol Processes (GLOMAP; Mann et al., 2010), which resulted in this HadGEM3 version in too little removal of the sulfate precursor SO_2 during the venting from the boundary layer to the free troposphere. The longer sulfate lifetime there explains the high column loadings.

In summary, we find that the Arctic is a region with particularly large relative differences between the models, both for the surface mass mixing ratios (with differences of more than an order of magnitude) as well as for the column loadings, and both for BC and sulfate. This must be related to differences in aerosol removal and lifetimes in the different models. We also found that, especially for sulfate, there can be an anticorrelation between simulated surface concentrations and column loadings. All this provides strong motivation to evaluate the models' performance in the Arctic, based on measurements taken both at the surface and aloft.

4 Observed and simulated BC and sulfate seasonality at Arctic surface measurement stations

We start our discussion of the annual cycles of aerosol concentrations with the example of BC at the Zeppelin station in Spitsbergen (Fig. 4). Monthly medians as well as the 25^{th} and 75^{th} percentile are calculated for every month based on hourly data for the two years 2008 and 2009. Maximum median eBC concentrations of 46 and 53 ng m^{-3} occur in March and April, while summer median values are only 2 to 3 ng m^{-3}. Some of the models capture this seasonality with high winter/spring values and much lower summer values quite well, although in most of these models BC reaches its highest values already in January. Only the CanAM4.2 model seems to capture the observed spring maximum. All models except WRF-Chem capture the very low summer values. OsloCTM2, TM4 and NorESM have smaller annual variation than observed. HadGEM3, which we have seen to produce lower BC surface concentrations than the other models in Fig. 3, strongly underestimates the measured eBC concentrations throughout the year. The variability of the modeled values within a month (described by the height of the bars) shows clear differences between the models. For instance, CAM5 simulates much less variable BC concentrations than CanAM4.2 and DEHM, or the measurements.

The eBC mass concentrations measured at the four other sites in the western Arctic are quite comparable to those at Zeppelin station, with monthly median values of about 20-80 ng m^{-3} in late winter/early spring and of less than 10 ng m^{-3} in summer/early fall (see Fig. 5). Only at the Tiksi station, which is closer to the main source regions of Arctic BC in high-latitude Eurasia (Hirdman et al., 2010), higher monthly median values were measured (more than 100 ng m^{-3} in winter/spring, about 20-40 ng m^{-3} in summer) and the annual mean (93 ng m^{-3}) is three times higher than the average for the other stations (32 ng m^{-3}). The seasonality of measured eBC is strongest at Alert where the summer concentrations are very low whereas the winter/spring concentrations are similar to the other sites in the western Arctic. This points to a deepening of the seasonal minimum with latitude. While the aerosol concentrations in the Arctic during late winter/early spring are comparable to remote regions further south, the concentrations in summer/early fall are lower because of the effective cleansing of the atmosphere (Garrett et al., 2010, 2011; Browse et al., 2012; Tunved et al., 2013) and less efficient transport (Stohl, 2006). The highest eBC concentrations were observed in January (Alert), February (Barrow), March (Pallas, Tiksi) or April (Zeppelin, Station Nord), with no clear dependence of the time of the maximum on latitude; however, the maximum occurred earlier at the two North American sites than at the other sites.

The models capture the Arctic BC concentrations with variable success (Fig. 5). There is clear progress since earlier studies (e.g. Shindell et al., 2008; Koch et al., 2009; AMAP, 2011), where it was reported that most models had a completely wrong seasonality and systematically underpredicted the Arctic Haze concentrations. In this study, most models do in fact capture the much higher concentrations in winter/spring than summer/fall, and some models can approximately reproduce the concentrations reached during the Arctic Haze season (see also Breider et al., 2014). However, as already seen for the Zeppelin station (Fig. 4) and the annual mean surface mass mixing ratios (Fig. 3), there is still a large variability between individual models, with seasonal median values varying by about an order of magnitude both in spring and summer even when excluding the most extreme models (see also Table 2). Seasonal mean concentrations during January to March are underestimated by up to a factor of 29 for individual models and by more than a factor 2 for the mean over all models, and only one model slightly overestimates the measured concentrations (Table 2). It is, however, important to keep in mind that measurements are also uncertain and could be biased high. By contrast, five models overpredict the low concentrations in summer, the most extreme model by an order of magnitude (Table 2). Some models (e.g., HadGEM3)

underpredict strongly throughout the year. For the sites in the western Arctic, the model deficiencies become worse with increasing latitude. For instance, at the northernmost site, Alert (82.5°N), all models underpredict for the full duration of the Arctic Haze season from January until April.

For Tiksi, data were not available for all models and the comparison is less direct as measurement data from July 2009-June 2010 were used. Nevertheless, it is clear that except for CanAM4.2 (which produces the highest modeled values at most sites) the models strongly underpredict for this site, especially in winter/spring. The most likely explanation for this is that the BC emissions in high-latitude Russia are underestimated in the ECLIPSE inventory. The alternative explanation – a too short BC lifetime in the models as suggested, for instance, by Samset et al. (2014) – would lead to even larger relative underestimates at the other more remote Arctic stations, which is not the case. It is difficult to know where exactly the missing sources are located. However, we find that in the ECLIPSE inventory the BC emissions in Norilsk (88.2°E, 69.3°N; population 170000) are zero. For SO_2, the ECLIPSE emissions for the year 2005 in the grid cells around Norilsk are 87 kt/yr, whereas AMAP (2006) report SO_2 emissions for the year 2002 of 2000 kt/yr. While we do not suggest that necessarily Norilsk emissions are responsible for the strong underestimation of BC concentrations at Tiksi, these discrepancies suggest that the high-latitude Russian emissions are underestimated and/or wrongly placed in the ECLIPSE inventory (as also in most other global emission inventories). In fact, we found that using a better proxy for the gridding of the non-ferrous smelter emissions substantially changed the distribution of sulfur emissions in Russia in a newly gridded ECLIPSE data set.

The seasonal cycle of sulfate at the monitoring stations is similar to that of BC, with a clear maximum during the Arctic Haze season and a minimum in summer/early fall (Fig. 6). However, the seasonal cycle at the northernmost stations is less strong than for BC, with about a factor 5 difference between spring and summer, compared to a factor 12 for BC (Table 2). This is probably due to the influence of biogenic sources of sulfate in summer (Quinn et al., 2002) and/or a weaker seasonality in the emissions (e.g., smelter emissions of SO_2 are probably relatively constant throughout the year).

The models have similar difficulties capturing the sulfate seasonality as they have for BC. Again, there is up to more than an order of magnitude difference between simulated seasonal median concentrations from different models, both in summer and in winter (Table 2). The

model differences in summer are in fact even larger than for BC, probably related to different treatment of natural sources, especially dimethyl sulfide emissions in the Arctic Ocean. There is a tendency that models that strongly underestimate BC concentrations also underestimate sulfate (e.g., HadGEM3 model) but the correlation between the two simulated species from the different models is quite low, especially in summer. For instance, ECHAM6-HAM2 underestimates BC by factors of 27 and 2 in winter and summer, but underestimates sulfate only by about 30% in winter and even overestimates sulfate by a factor of 3.5 in summer. As seen in Fig. 2 and 3, ECHAM6-HAM2 simulates relatively high surface concentrations of sulfate but low total column loadings, both at source and Arctic latitudes.

Most models underpredict values strongest at the northernmost station (Alert), which is consistent with the BC results (compare Figs. 5 and 6). The CanAM4.2 model, which had some of the highest BC concentrations, also gives the highest sulfate values (Table 2). CanAM4.2 is also the only model matching the high measured values at Alert and Barrow in spring.

At Pallas, the lowest-latitude station in this comparison, all the models except for CanAM4.2 severely underestimate sulfate (Fig. 6), although they tend to overestimate BC in spring there. One likely reason for the sulfate underestimation is the proximity of the Pallas station to the Kola peninsula, where metal smelters are a strong source of sulfur. According to AMAP (2006), SO_2 emissions in Nikel, Zapolyarnyy and Monchegorsk together were about 170 kt/yr in the year 2002. In the ECLIPSE inventory used for this study the SO_2 emissions in these areas are, however, only about 33 kt/yr in total for the year 2005. Similar underestimates were in fact reported also for other emission inventories for this region (Prank et al., 2010). Strong underestimation of the SO_2 emissions from metal smelting in the Kola peninsula is therefore a likely explanation why almost all models underestimate sulfate at Pallas so strongly.

5 Vertical Profiles

Figure 7 summarizes all rBC data from the ARCTAS and ARCPAC campaigns in spring 2008. Median concentrations are shown as a function of latitude (binned into 10° intervals) both for lower (<3 km) and higher (>3 km) altitudes, and as a function of altitude both for the high Arctic (>70°N) and lower latitudes. As the campaigns focussed on the Arctic, data south of 60°N are somewhat scarce. The models were sampled in their grid box containing a measurement location and at the time of a measurement and were subsequently binned in the same way as the measurement data to allow a direct comparison. For the free-running climate

models, the same procedure was used, albeit with the caveat that the simulated meteorological situation at the measurement time does not correspond to the real conditions.

For the low-altitude (<3 km) bin, the highest median rBC values were measured (see Fig. 7, 2nd row) at 35°N and 55°N, with a substantial drop of the concentrations towards higher latitudes. The mid-latitude maximum reflects the location of the BC sources in North America, where ARCTAS and ARCPAC were conducted. Above 3 km, the highest median rBC concentrations were measured further north, at 60°N, and the concentrations drop less strongly towards the North Pole than at lower altitudes. This is due to quasi-isentropic lifting occurring together with northward transport (Stohl, 2006). All models, except CanAM4.2, systematically underestimate the measured values for both altitude bins and for all latitudes, and they also underestimate the measured rBC variability. However, most of the models simulate a decrease of the concentrations with latitude that is consistent with the measured latitude dependence.

When plotted as a function of altitude, the measured values peak in the 4-5 km altitude bin, both for sub-Arctic and Arctic latitudes. The models, except for CanAM4.2, underestimate the measured median values throughout the entire depth of the profile. Some of the models, mainly those driven by observed meteorology, capture the BC maximum in the mid-troposphere in the Arctic. However, the lower-latitude 4-5 km maximum is hardly captured by any of the models. One likely reason for the modeling problems is the strong biomass burning activity during spring 2008, which influenced a substantial fraction of the measurement data (Warneke et al., 2010; Brock et al., 2011). Even though this should be reflected in the GFED emission data for 2008, it seems possible that the emissions are underestimated (REF? – paper by Sarah Monks??). Furthermore, as some of the flights targeted biomass burning plumes specifically, the influence of the biomass burning may be enhanced in the measurement data compared to the models, especially if the models did not capture the plume transport well enough and thus potentially simulated the biomass burning plumes at other locations than observed. This sampling bias is expected to be particularly strong for the CCMs which are not driven by observed meteorological fields.

Comparisons like in Fig. 7 were performed also for the other aircraft campaigns. For the sake of brevity, we further aggregate the data and only show results for latitudes north of 70°N and for median values below and above 3 km altitude (Fig. 8). For spring 2008, the aggregate plots for BC (Fig. 8e-f) show even more clearly than Fig. 7 that all models except CanAM4.2

underestimate the measured rBC concentrations both at low and high altitudes. The spring 2009 PAMARCMiP campaign, however, shows a different picture (Fig. 8c-d). This campaign was influenced very little by biomass burning (REF?). The measured median rBC mass concentrations at low (high) altitudes were about a factor two (three) lower than for the spring 2008 campaigns. Most models also simulated lower median BC concentrations than a year earlier but the modeled reductions were less pronounced than the measured ones and, thus, about half of the models under- and the other half overestimated the measured median values. The vertical gradient of measured BC was also different in 2008 and in 2009. While in spring 2008, the concentrations above 3 km were higher than those below, the opposite was true in spring 2009, likely because of the weaker biomass burning influence in 2009. This feature can be seen very clearly in the vertical profiles shown in Fig. 9 and it is not well captured by the models, most of which showed a relatively flat vertical BC distribution.

The concentrations measured by the ARCTAS summer campaign in 2008 are much lower than in spring 2008 and 2009, both at low and high altitudes (Fig. 8g-h), which is in agreement with the seasonality seen at the surface stations. Some of the models under- and others overestimate the measured concentrations, with the majority of the models overestimating, especially below 3 km, suggesting that summer fire emissions are overestimated since many of the flights took place near to Canadian boreal fires. The mean values, averaged over all models, are about two times (three times) as high as the measurements for altitudes above (below) 3 km. Some of the models reproduce the measured rBC maximum at 6 km (Fig. 9).

The HIPPO campaign in fall 2009 (Fig. 8i-j) was conducted about one month after the seasonal minimum at most surface sites and measured very low rBC mass concentrations, which is consistent with the surface observations. Most of the models overestimate the measured concentrations throughout the entire vertical profile (Fig. 9).

The HIPPO campaign in January 2009 (Fig. 8a-b) measured strong altitude differences: moderately high rBC mass concentrations up to 3 km, but the lowest concentrations of all campaigns above. This feature is well captured by some of the models (Fig. 9). The lack of high concentrations aloft is likely related to the minimal influence of biomass burning at this time of the year.

Overall, the aircraft measurements confirm the BC seasonality measured at the surface stations. They also confirm that most models underestimate the concentrations in spring (at

least for the year 2008) but many models overestimate the concentrations in summer and fall. It thus seems that models produce a too weak BC seasonality throughout the depth of the troposphere. However, for the year as a whole there is a tendency towards model overestimates, in contrast to the surface sites. Even stronger model overestimates downwind of Asia over the Pacific??, especially in the upper troposphere, were recently reported by Samset et al. (2014) who suggested that the BC lifetime in the models is too long. However, a uniform reduction of BC lifetime in our models would lead to strong underestimates of the BC concentrations at the Arctic measurement stations and even the Arctic aircraft comparisons only support at most a very moderate BC lifetime reduction. Of course, regional and/or vertical differences in the model lifetime biases could explain the contrasting findings of our study and Samset et al. (2014).

For sulfate, measured median concentrations in the Arctic during spring 2008 were lower above 3 km than below 3 km (Fig. 10a-b). All models, except CanAM4.2, strongly underestimate the measured sulfate concentrations, some models by more than an order of magnitude. This is consistent with the findings from the surface station comparisons (Fig. 6, Table 2). The models also do not give a consistent picture of the vertical distribution of sulfate, with some models correctly simulating lower concentrations above 3 km than below but others giving the opposite result. The model underestimates for sulfate are likely not related to a sampling bias towards frequent encounters of biomass burning plumes, as biomass burning plumes are relatively poor in sulfate (e.g. Brock et al., 2011). Instead, the underestimation suggests missing sulfur sources or a too quick removal of sulfate from the atmosphere. Indeed, the latter would be consistent with the suggestion of Kristiansen et al. (2012) that sulfate lifetimes in models are too short in spring (in the lower troposphere?).

During summer 2008 (Fig. 10c-d), the measured median sulfate concentrations were about a factor 4-6 lower than in spring 2008, consistent with the seasonality measured at surface sites. Median concentrations above and below 3 km are very similar. The models have very large differences in their simulated sulfate concentrations, with some models over- and others underestimating the measured concentrations. This is again consistent with the findings from the surface site comparison (Fig. 6, Table 2).

6 Station vs. low-altitude aircraft measurements

Contrary to the year-round station measurement programs, the aircraft campaigns sample the atmosphere only during a limited time period and their representativeness with regard to climatological means may be questioned. Furthermore, from the aircraft measurements we have seen that spring 2008 and 2009 had very different measured rBC concentrations, and modeling problems were larger for spring 2008 when there was intensive biomass burning and flaring influence in the Arctic. A valid question is therefore whether the surface measurements show the same differences between 2008 and 2009.

To investigate how consistent a picture the aircraft campaigns give vis a vis the station measurements, we compare all aircraft data from the lowest 3 km and lowest 1 km to the values obtained from the surface stations for the same months (Fig. 11). Selecting data only for even lower altitudes is problematic as the data coverage becomes very poor. In Fig. 11, we also show the station measurements obtained for the years 2008 and 2009 separately. For eBC, the measurements obtained for the same month at the different stations and during different years are (with a few exceptions such as Barrow in January 2008) quite comparable with each other. In particular, April 2008 did not show higher eBC values than April 2009. This is consistent with the finding that the biomass burning layers in 2008 did not extend to the surface (Brock et al., 2011). The models underestimate the high eBC values measured in spring at the surface about equally in years with (2008) and without (2009) strong biomass burning. The aircraft rBC measurements for all campaigns show consistently lower values than the eBC measurements at the ground, except for the HIPPO campaign in January 2009 where, however, the data coverage particularly below 1 km is poor. It is possible that the BC concentrations show a strong gradient in the lowest 1 km and that surface concentrations are indeed systematically higher than concentrations just aloft. However, an alternative explanation could be that the rBC measurements are biased low against the eBC measurements, given the different measurement techniques used.

For sulfate (Fig. 12) the measurements show a much larger relative variability than for BC, both between stations and between the two different years. For instance, the 25th percentile of the sulfate concentrations at Alert in January 2009 is higher than the 75th percentile of the other stations and also of Alert in January 2008. On the other hand, the sulfate concentrations measured during the two available flight campaigns in spring and summer 2008 are not systematically different from those measured at the stations, although the median

concentration in summer 2008 is somewhat lower than at the stations. This is consistent with the eBC/rBC differences.

7 Sulfate/BC correlations

Figure 13 shows correlation plots between monthly mean sulfate and eBC for the measurements and the models sampled at the different stations. The slopes of the regression lines shown in Fig. 13 are reported in Table 3. For the observations, they are very similar: 10.1, 8.4 and 8.9 ng[SO_4] m^{-3} / ng[BC] m^{-3} for Alert, Pallas and Zeppelin, respectively. For Barrow, where the correlation is not significant because of two eBC-rich outlier data points, the slope is smaller (6.4 ng[SO_4] m^{-3} / ng[BC] m^{-3}). Without these two data points, however, the slope becomes very similar to the other stations. The strong correlation between sulfate and eBC and the similarity of the slopes suggests that the sources contributing to the measurements at the different stations are similar and that the removal of sulfate and eBC is highly correlated, which would be expected for internally mixed aerosol as it is typical for the Arctic.

Most of the models, on the other hand, show much weaker correlation between sulfate and BC and some of the models have no significant correlation at all. Exceptions are DEHM, CAM5 and WRF-Chem which show mainly significant correlations, and slopes that are comparable at the different stations and which are also quite similar to the observed slopes. This suggests that, with the given emissions, it is possible to reproduce the observed correlations. The lack of correlation between sulfate and BC in the other models – in disagreement with the observations – therefore suggests that they treat the two species very differently, probably having (a too large fraction of) the aerosol as externally mixed. Correlations could also be degraded by a probably too strong influence of biogenic (dimethyl sulfide) emissions from the oceans or factors influencing SO_2 to sulphate conversion such as the level of oxidants in the models.

The SO_2 (converted to sulfate) to BC emission ratios of anthropogenic emissions in the ECLIPSE inventory is 25 globally and 40 north of 50°N. For the GFED biomass burning emissions the emission ratio is only 1.7 globally and 2.5 north of 50°N, and for the sum of anthropogenic and biomass burning emissions, we obtain ratios of 19 globally and 25 north of 50°N. The mean observed slopes of the observations (9.1 ng[SO_4] m^{-3} / ng[BC] m^{-3}) and the slopes modeled by DEHM (5.4 ng[SO_4] m^{-3} / ng[BC] m^{-3}), CAM5 (9.9 ng[SO_4] m^{-}

^{3} / ng[BC] m^{-3}) and WRF-Chem (8.5 ng[SO_4] m^{-3} / ng[BC] m^{-3}) are much lower than the emission ratio of anthropogenic emissions in the ECLIPSE inventory and they are also lower than the emission ratio for mixed anthropogenic and biomass burning emissions. This suggests that biomass burning emissions are relatively more important in the Arctic than elsewhere, that there are missing BC sources (or sulphur emissions are overestimated), and/or that there exists a mechanism that enriches aerosols in BC relative to sulfate in the Arctic atmosphere. The latter could be related to the hydrophobic nature of BC immediately after it is emitted.

8 Conclusions

Based on our study, we can draw the following conclusions:

- The simulation of BC concentrations in the Arctic has improved compared to earlier studies that have compared models and observations (e.g. Shindell et al., 2008; Koch et al., 2009; AMAP, 2011). Nevertheless, the aerosol seasonality at the surface is still too weak in most models. Concentrations of eBC and sulfate averaged over three (four for eBC) surface sites in the western Arctic are underestimated in winter/spring in all but one model (model means for January-March underestimated by 57% and 41% for BC and sulfate), whereas concentrations in summer are overestimated in the model mean (by 60% and 33% for July-September), but with over- as well as underestimates present in individual models.
- For the aircraft campaigns, the models overestimated measured rBC during all seasons except for spring and throughout the depth of the troposphere. Only in spring 2009, no overestimate was found, and in spring 2008 the models underestimated both rBC and sulfate strongly. For rBC, this could have been due to underestimation of the strong influence of biomass burning emissions observed during that campaign (flaring?) What about other processes – scavenging, model resolution etc?.
- The largest eBC underestimates are found for the station Tiksi, which is closest to potential Russian source regions and where the annual mean eBC concentration is three times higher than the average annual mean for all other stations. This suggests an underestimate of BC sources in Russia in the emission inventory used, even though this inventory contains gas flaring as an important BC source there.

- We found a strong correlation between observed sulfate and eBC with consistent sulfate/eBC slopes for all Arctic stations. This indicates that the sources contributing to sulfate and BC throughout the Arctic are similar and that the aerosols are internally mixed and undergo similar removal. However, only three models reproduced this finding, whereas sulfate and BC are weakly correlated in the other models.
- We found that overall, no class of models (e.g., CTMs, CCMs) performed substantially better than the others and differences are largely due to the treatment of aerosol removal in the models.

Acknowledgements

The research leading to these results has received funding from the European Union Seventh Framework Programme (FP7/2007-2013) under grant agreement no 282688 – ECLIPSE. Some of the work was conducted for and funded by the Arctic Monitoring and Assessment Programme (AMAP). ECMWF gave access to their meteorological data. French authors also acknowledge support from the CLIMSLIP-ANR project and computer resources provided by IDRIS.

Environment Canada (Sangeeta Sharma) provided the sulfate data from Alert.

Andreas Massling (Aarhus University, Department of Environmental Science) provided Station Nord data.

WMO GAW stations.

Alert sulfate, Alert eBC, Zeppelin (Tunved?), Tiksi, and all contributors to the ARCTAS, ARCPAC, HIPPO, and PAMARCMiP campaigns.

We acknowledge the use of HIPPO data products downloaded from http://hippo.ornl.gov/dataaccess

References

Allen, R. J., and Landuyt, W.: The vertical distribution of black carbon in CMIP5models: Comparison to observations and the importance of convective transport, Journal of Geophysical Research-Atmospheres, 119, 4808-4835, 10.1002/2014jd021595, 2014.

Amann, M., Klimont, Z., and Wagner, F.: Regional and global emissions of air pollutants: Recent trends and future scenarios, Annual Review of Environment and Resources, 38, 31-55, 2013.

AMAP, 2006. AMAP Assessment 2006: Acidifying Pollutants, Arctic Haze, and Acidification in the Arctic. Arctic Monitoring and Assessment Programme (AMAP), Oslo, Norway. xii+112 pp.

Andersson, C., Langner, J., and Bergstrom, R.: Interannual variation and trends in air pollution over Europe due to climate variability during 1958-2001 simulated with a regional CTM coupled to the ERA40 reanalysis, Tellus Series B-Chemical and Physical Meteorology, 59, 77-98, 10.1111/j.1600-0889.2006.00196.x, 2007.

Bahreini, R., Dunlea, E. J., Matthew, B. M., Simons, C., Docherty, K. S., DeCarlo, P. F., Jimenez, J. L., Brock, C. A., and Middlebrook, A. M.: Design and operation of a pressure-controlled inlet for airborne sampling with an aerodynamic aerosol lens, Aerosol Science and Technology, 42, 465-471, 10.1080/02786820802178514, 2008.

Bentsen, M., Bethke, I., Debernard, J. B., Iversen, T., Kirkevag, A., Seland, O., Drange, H., Roelandt, C., Seierstad, I. A., Hoose, C., and Kristjansson, J. E.: The Norwegian Earth System Model, NorESM1-M - Part 1: Description and basic evaluation of the physical climate, Geoscientific Model Development, 6, 687-720, 10.5194/gmd-6-687-2013, 2013.

Bond, T. C., Streets, D. G., Yarber, K. F., Nelson, S. M., Woo, J. H., and Klimont, Z.: A technology-based global inventory of black and organic carbon emissions from combustion, Journal of Geophysical Research-Atmospheres, 109, 10.1029/2003jd003697, 2004.

Bond, T. C., and Bergstrom, R. W.: Light absorption by carbonaceous particles: An investigative review, Aerosol Science and Technology, 40, 27-67, 10.1080/02786820500421521, 2006.

Brandt, J., Silver, J. D., Frohn, L. M., Geels, C., Gross, A., Hansen, A. B., Hansen, K. M., Hedegaard, G. B., Skjoth, C. A., Villadsen, H., Zare, A., and Christensen, J. H.: An integrated

model study for Europe and North America using the Danish Eulerian Hemispheric Model with focus on intercontinental transport of air pollution, Atmospheric Environment, 53, 156-176, 10.1016/j.atmosenv.2012.01.011, 2012.

Breider, T. J., Mickley, L. J., Jacob, D. J., Wang, Q., Fisher, J. A., Chang, R. Y. W., and Alexander, B.: Annual distributions and sources of Arctic aerosol components, aerosol optical depth, and aerosol absorption, Journal of Geophysical Research-Atmospheres, 119, 4107-4124, 2014.

Brock, C. A., Cozic, J., Bahreini, R., Froyd, K. D., Middlebrook, A. M., McComiskey, A., Brioude, J., Cooper, O. R., Stohl, A., Aikin, K. C., de Gouw, J. A., Fahey, D. W., Ferrare, R. A., Gao, R. S., Gore, W., Holloway, J. S., Hubler, G., Jefferson, A., Lack, D. A., Lance, S., Moore, R. H., Murphy, D. M., Nenes, A., Novelli, P. C., Nowak, J. B., Ogren, J. A., Peischl, J., Pierce, R. B., Pilewskie, P., Quinn, P. K., Ryerson, T. B., Schmidt, K. S., Schwarz, J. P., Sodemann, H., Spackman, J. R., Stark, H., Thomson, D. S., Thornberry, T., Veres, P., Watts, L. A., Warneke, C., and Wollny, A. G.: Characteristics, sources, and transport of aerosols measured in spring 2008 during the aerosol, radiation, and cloud processes affecting Arctic Climate (ARCPAC) Project, Atmospheric Chemistry and Physics, 11, 2423-2453, 10.5194/acp-11-2423-2011, 2011.

Browse, J., K. S. Carslaw, S. Arnold, K. J. Pringle and O. Boucher, The scavenging processes controlling the seasonal cycle in Arctic sulfate and black carbon aerosol, Atmospheric Chemistry and Physics 12, 6775 – 6798, 2012.

Christensen, J. H.: The Danish Eulerian hemispheric model - A three-dimensional air pollution model used for the Arctic, Atmospheric Environment, 31, 4169-4191, 10.1016/s1352-2310(97)00264-1, 1997.

Eleftheriadis, K., Vratolis, S., and Nyeki, S.: Aerosol black carbon in the European Arctic: Measurements at Zeppelin station, Ny-Alesund, Svalbard from 1998-2007, Geophysical Research Letters, 36, 5, 10.1029/2008gl035741, 2009.

Fisher, J. A., Jacob, D. J., Wang, Q., Bahreini, R., Carouge, C. C., Cubison, M. J., Dibb, J. E., Diehl, T., Jimenez, J. L., Leibensperger, E. M., Lu, Z., Meinders, M. B. J., Pye, H. O. T., Quinn, P. K., Sharma, S., Streets, D. G., van Donkelaar, A., and Yantosca, R. M.: Sources, distribution, and acidity of sulfate-ammonium aerosol in the Arctic in winter-spring, Atmospheric Environment, 45, 7301-7318, 10.1016/j.atmosenv.2011.08.030, 2011.

Flanner, M. G., Zender, C. S., Hess, P. G., Mahowald, N. M., Painter, T. H., Ramanathan, V., and Rasch, P. J.: Springtime warming and reduced snow cover from carbonaceous particles, Atmospheric Chemistry and Physics, 9, 2481-2497, 2009.

Garrett, T. J., Zhao, C., and Novelli, P. C.: Assessing the relative contributions of transport efficiency and scavenging to seasonal variability in Arctic aerosol, Tellus Series B-Chemical and Physical Meteorology, 62, 190-196, 10.1111/j.1600-0889.2010.00453.x, 2010.

Garrett, T. J., Brattstrom, S., Sharma, S., Worthy, D. E. J., and Novelli, P.: The role of scavenging in the seasonal transport of black carbon and sulfate to the Arctic, Geophysical Research Letters, 38, 10.1029/2011gl048221, 2011.

GEA (2012), Global Energy Assessment: Toward a Sustainable Future, Cambridge University Press, UK.

Gong, S. L., Zhao, T. L., Sharma, S., Toom-Sauntry, D., Lavoue, D., Zhang, X. B., Leaitch, W. R., and Barrie, L. A.: Identification of trends and interannual variability of sulfate and black carbon in the Canadian High Arctic: 1981-2007, Journal of Geophysical Research-Atmospheres, 115, 9, 10.1029/2009jd012943, 2010.

Hewitt, H. T., Copsey, D., Culverwell, I. D., Harris, C. M., Hill, R. S. R., Keen, A. B., McLaren, A. J., and Hunke, E. C.: Design and implementation of the infrastructure of HadGEM3: the next-generation Met Office climate modelling system, Geoscientific Model Development, 4, 223-253, 10.5194/gmd-4-223-2011, 2011.

Hirdman, D., J. F. Burkhart, H. Sodemann, S. Eckhardt, A. Jefferson, P. K. Quinn, S. Sharma, J. Ström and A. Stohl, Long-term trends of black carbon and sulphate aerosol in the Arctic: changes in atmospheric transport and source region emissions, Atmospheric Chemistry and Physics 10, 9351 – 9368, 2010.

Huang, L., Gong, S. L., Jia, C. Q., and Lavoue, D.: Relative contributions of anthropogenic emissions to black carbon aerosol in the Arctic, Journal of Geophysical Research-Atmospheres, 115, 11, 10.1029/2009jd013592, 2010.

Hyvarinen, A. P., Kolmonen, P., Kerminen, V. M., Virkkula, A., Leskinen, A., Komppula, M., Hatakka, J., Burkhart, J., Stohl, A., Aalto, P., Kulmala, M., Lehtinen, K. E. J., Viisanen, Y., and Lihavainen, H.: Aerosol black carbon at five background measurement sites over Finland, a gateway to the Arctic, Atmospheric Environment, 45, 4042-4050, 10.1016/j.atmosenv.2011.04.026, 2011.

Jacob, D. J., Crawford, J. H., Maring, H., Clarke, A. D., Dibb, J. E., Emmons, L. K., Ferrare, R. A., Hostetler, C. A., Russell, P. B., Singh, H. B., Thompson, A. M., Shaw, G. E., McCauley, E., Pederson, J. R., and Fisher, J. A.: The Arctic Research of the Composition of the Troposphere from Aircraft and Satellites (ARCTAS) mission: design, execution, and first results, Atmospheric Chemistry and Physics, 10, 5191-5212, 10.5194/acp-10-5191-2010, 2010.

Jacobson, M. Z.: Climate response of fossil fuel and biofuel soot, accounting for soot's feedback to snow and sea ice albedo and emissivity, Journal of Geophysical Research-Atmospheres, 109, 10.1029/2004jd004945, 2004.

Kanakidou, M., Duce, R. A., Prospero, J. M., Baker, A. R., Benitez-Nelson, C., Dentener, F. J., Hunter, K. A., Liss, P. S., Mahowald, N., Okin, G. S., Sarin, M., Tsigaridis, K., Uematsu, M., Zamora, L. M., and Zhu, T.: Atmospheric fluxes of organic N and P to the global ocean, Global Biogeochemical Cycles, 26, 10.1029/2011gb004277, 2012.

Klimont, Z., Smith, S. J., and Cofala, J.: The last decade of global anthropogenic sulfur dioxide: 2000-2011 emissions, Environmental Research Letters, 8, 10.1088/1748-9326/8/1/014003, 2013.

Klimont, Z., Kupiainen, K., Heyes, Ch., Purohit, P., Cofala, J., Rafaj, P., Borken-Kleefeld, J., Schoepp, W. Global anthropogenic emissions of particulate matter. In preparation, 2015a.

Klimont, Z., Hoglund, L., Heyes, Ch., Rafaj, P., Schoepp, W., Cofala, J., Borken-Kleefeld, J., Purohit, P., Kupiainen, K., Winiwarter, W., Amann, M., Zhao, B., Wang, S.X., Bertok, I., and Sander, R. Global scenarios of air pollutants and methane: 1990-2050. In preparation, 2015b.

Koch, D., Schulz, M., Kinne, S., McNaughton, C., Spackman, J. R., Balkanski, Y., Bauer, S., Berntsen, T., Bond, T. C., Boucher, O., Chin, M., Clarke, A., De Luca, N., Dentener, F., Diehl, T., Dubovik, O., Easter, R., Fahey, D. W., Feichter, J., Fillmore, D., Freitag, S., Ghan, S., Ginoux, P., Gong, S., Horowitz, L., Iversen, T., Kirkevag, A., Klimont, Z., Kondo, Y., Krol, M., Liu, X., Miller, R., Montanaro, V., Moteki, N., Myhre, G., Penner, J. E., Perlwitz, J., Pitari, G., Reddy, S., Sahu, L., Sakamoto, H., Schuster, G., Schwarz, J. P., Seland, O., Stier, P., Takegawa, N., Takemura, T., Textor, C., van Aardenne, J. A., and Zhao, Y.: Evaluation of black carbon estimations in global aerosol models, Atmospheric Chemistry and Physics, 9, 9001-9026, 2009.

Kristiansen, N. I., Stohl, A., and Wotawa, G.: Atmospheric removal times of the aerosol-bound radionuclides ^{137}Cs and ^{131}I measured after the Fukushima Dai-ichi nuclear accident – a constraint for air quality and climate models, Atmos. Chem. Phys., 12, 10759-10769, doi:10.5194/acp-12-10759-2012, 2012.

Lamarque, J. F., Bond, T. C., Eyring, V., Granier, C., Heil, A., Klimont, Z., Lee, D., Liousse, C., Mieville, A., Owen, B., Schultz, M. G., Shindell, D., Smith, S. J., Stehfest, E., Van Aardenne, J., Cooper, O. R., Kainuma, M., Mahowald, N., McConnell, J. R., Naik, V., Riahi, K., and van Vuuren, D. P.: Historical (1850-2000) gridded anthropogenic and biomass burning emissions of reactive gases and aerosols: methodology and application, Atmospheric Chemistry and Physics, 10, 7017-7039, 10.5194/acp-10-7017-2010, 2010.

Law, K. S., and Stohl, A.: Arctic air pollution: Origins and impacts, Science, 315, 1537-1540, 10.1126/science.1137695, 2007.

Liu, J. F., Fan, S. M., Horowitz, L. W., and Levy, H.: Evaluation of factors controlling long-range transport of black carbon to the Arctic, Journal of Geophysical Research-Atmospheres, 116, 15, 10.1029/2010jd015145, 2011.

Lund, M. T., and Berntsen, T.: Parameterization of black carbon aging in the OsloCTM2 and implications for regional transport to the Arctic, Atmospheric Chemistry and Physics, 12, 6999-7014, 10.5194/acp-12-6999-2012, 2012.

Mann, G. W., Carslaw, K. S., Spracklen, D. V., Ridley, D. A., Manktelow, P. T., Chipperfield, M. P., Pickering, S. J., and Johnson, C. E.: Description and evaluation of GLOMAP-mode: a modal global aerosol microphysics model for the UKCA composition-climate model, Geosci. Model Dev., 3, 519-551, doi:10.5194/gmd-3-519-2010, 2010.

Menegoz, M., Voldoire, A., Teyssedre, H., Salas y Melia, D., Peuch, V. H., and Gouttevin, I.: How does the atmospheric variability drive the aerosol residence time in the Arctic region?, Tellus Series B-Chemical and Physical Meteorology, 64, 10.3402/tellusb.v64i0.11596, 2012.

Myhre, G., Berglen, T. F., Johnsrud, M., Hoyle, C. R., Berntsen, T. K., Christopher, S. A., Fahey, D. W., Isaksen, I. S. A., Jones, T. A., Kahn, R. A., Loeb, N., Quinn, P., Remer, L., Schwarz, J. P., and Yttri, K. E.: Modelled radiative forcing of the direct aerosol effect with multi-observation evaluation, Atmospheric Chemistry and Physics, 9, 1365-1392, 10.5194/acp-9-1365-2009, 2009.

Myhre, G., D. Shindell, F.-M. Bréon, W. Collins, J. Fuglestvedt, J. Huang, D. Koch, J.-F. Lamarque, D. Lee, B. Mendoza, T. Nakajima, A. Robock, G. Stephens, T. Takemura and H. Zhang: Anthropogenic and Natural Radiative Forcing. In: Climate Change 2013: The Physical Science Basis. Contribution of Working Group I to the Fifth Assessment Report of the Intergovernmental Panel on Climate Change, Stocker, T.F., D. Qin, G.-K. Plattner, M. Tignor, S.K. Allen, J. Boschung, A. Nauels, Y. Xia, V. Bex and P.M. Midgley (eds.), Cambridge University Press, Cambridge, United Kingdom and New York, NY, USA, 2013.

Myriokefalitakis, S., Tsigaridis, K., Mihalopoulos, N., Sciare, J., Nenes, A., Kawamura, K., Segers, A., and Kanakidou, M.: In-cloud oxalate formation in the global troposphere: a 3-D modeling study, Atmospheric Chemistry and Physics, 11, 5761-5782, 10.5194/acp-11-5761-2011, 2011.

Nguyen, Q. T., Skov, H., Sorensen, L. L., Jensen, B. J., Grube, A. G., Massling, A., Glasius, M., and Nojgaard, J. K.: Source apportionment of particles at Station Nord, North East Greenland during 2008-2010 using COPREM and PMF analysis, Atmospheric Chemistry and Physics, 13, 35-49, 10.5194/acp-13-35-2013, 2013.

Prank, M., Sofiev, M., Denier van der Gon, H. A. C., Kaasik, M., Ruuskanen, T. M., and Kukkonen, J.: A refinement of the emission data for Kola Peninsula based on inverse dispersion modelling, Atmos. Chem. Phys., 10, 10849-10865, doi:10.5194/acp-10-10849-2010, 2010.

Quinn, P. K., Miller, T. L., Bates, T. S., Ogren, J. A., Andrews, E., and Shaw, G. E.: A 3-year record of simultaneously measured aerosol chemical and optical properties at Barrow, Alaska, Journal of Geophysical Research-Atmospheres, 107, 10.1029/2001jd001248, 2002.

Quinn, P. K., Shaw, G., Andrews, E., Dutton, E. G., Ruoho-Airola, T., and Gong, S. L.: Arctic haze: current trends and knowledge gaps, Tellus Series B-Chemical and Physical Meteorology, 59, 99-114, 10.1111/j.1600-0889.2006.00238.x, 2007.

Quinn, P. K., Bates, T. S., Baum, E., Doubleday, N., Fiore, A. M., Flanner, M., Fridlind, A., Garrett, T. J., Koch, D., Menon, S., Shindell, D., Stohl, A., and Warren, S. G.: Short-lived pollutants in the Arctic: their climate impact and possible mitigation strategies, Atmospheric Chemistry and Physics, 8, 1723-1735, 10.5194/acp-8-1723-2008, 2008.

Ramanathan, V., and Carmichael, G.: Global and regional climate changes due to black carbon, Nature Geoscience, 1, 221-227, 10.1038/ngeo156, 2008.

Riahi, K. et al. (2012), Chapter 17 - Energy Pathways for Sustainable Development, in Global Energy Assessment - Toward a Sustainable Future, pp. 1203–1306, Cambridge University Press, Cambridge, UK and New York, NY, USA and the International Institute for Applied Systems Analysis, Laxenburg, Austria. [online] Available from: www.globalenergyassessment.org

Robertson, L., Langner, J., and Engardt, M.: An Eulerian limited-area atmospheric transport model, Journal of Applied Meteorology, 38, 190-210, 10.1175/1520-0450(1999)038<0190:aelaat>2.0.co;2, 1999.

Samset, B. H., Myhre, G., Herber, A., Kondo, Y., Li, S.-M., Moteki, N., Koike, M., Oshima, N., Schwarz, J. P., Balkanski, Y., Bauer, S. E., Bellouin, N., Berntsen, T. K., Bian, H., Chin, M., Diehl, T., Easter, R. C., Ghan, S. J., Iversen, T., Kirkevåg, A., Lamarque, J.-F., Lin, G., Liu, X., Penner, J. E., Schulz, M., Seland, Ø., Skeie, R. B., Stier, P., Takemura, T., Tsigaridis, K., and Zhang, K.: Modelled black carbon radiative forcing and atmospheric lifetime in AeroCom Phase II constrained by aircraft observations, Atmos. Chem. Phys., 14, 12465-12477, doi:10.5194/acp-14-12465-2014, 2014.

Schwarz, J. P., Spackman, J. R., Gao, R. S., Watts, L. A., Stier, P., Schulz, M., Davis, S. M., Wofsy, S. C., and Fahey, D. W.: Global-scale black carbon profiles observed in the remote atmosphere and compared to models, Geophys. Res. Lett., 37, L18812, doi:10.1029/2010GL044372, 2010.

Schwarz, J. P., Samset, B. H., Perring, A. E., Spackman, J. R., Gao, R. S., Stier, P., Schulz, M., Moore, F. L., Ray, E. A., and Fahey, D. W.: Global-scale seasonally resolved black carbon vertical profiles over the Pacific, Geophys. Res. Lett., 40, 5542–5547, doi:10.1002/2013GL057775, 2013.

Sharma, S., Andrews, E., Barrie, L. A., Ogren, J. A., and Lavoue, D.: Variations and sources of the equivalent black carbon in the high Arctic revealed by long-term observations at Alert and Barrow: 1989-2003, Journal of Geophysical Research-Atmospheres, 111, 10.1029/2005jd006581, 2006.

Sharma, S., Ishizawa, M., Chan, D., Lavoue, D., Andrews, E., Eleftheriadis, K., and Maksyutov, S.: 16-year simulation of Arctic black carbon: Transport, source contribution, and sensitivity analysis on deposition, Journal of Geophysical Research-Atmospheres, 118, 943-964, 10.1029/2012jd017774, 2013.

Shaw, G. E.: The Arctic Haze Phenomenon, Bulletin of the American Meteorological Society, 76, 2403 – 2412, 1995.

Shindell, D., and Faluvegi, G.: Climate response to regional radiative forcing during the twentieth century, Nature Geoscience, 2, 294-300, 10.1038/ngeo473, 2009.

Shindell, D. T., Chin, M., Dentener, F., Doherty, R. M., Faluvegi, G., Fiore, A. M., Hess, P., Koch, D. M., MacKenzie, I. A., Sanderson, M. G., Schultz, M. G., Schulz, M., Stevenson, D. S., Teich, H., Textor, C., Wild, O., Bergmann, D. J., Bey, I., Bian, H., Cuvelier, C., Duncan, B. N., Folberth, G., Horowitz, L. W., Jonson, J., Kaminski, J. W., Marmer, E., Park, R., Pringle, K. J., Schroeder, S., Szopa, S., Takemura, T., Zeng, G., Keating, T. J., and Zuber, A.: A multi-model assessment of pollution transport to the Arctic, Atmospheric Chemistry and Physics, 8, 5353-5372, 2008.

Skeie, R. B., Berntsen, T. K., Myhre, G., Tanaka, K., Kvalevag, M. M., and Hoyle, C. R.: Anthropogenic radiative forcing time series from pre-industrial times until 2010, Atmospheric Chemistry and Physics, 11, 11827-11857, 10.5194/acp-11-11827-2011, 2011a.

Skeie, R. B., Berntsen, T., Myhre, G., Pedersen, C. A., Ström, J., Gerland, S., and Ogren, J. A.: Black carbon in the atmosphere and snow, from pre-industrial times until present, Atmos. Chem. Phys., 11, 6809-6836, doi:10.5194/acp-11-6809-2011, 2011b.

Stevens, B., Giorgetta, M., Esch, M., Mauritsen, T., Crueger, T., Rast, S., Salzmann, M., Schmidt, H., Bader, J., Block, K., Brokopf, R., Fast, I., Kinne, S., Kornblueh, L., Lohmann, U., Pincus, R., Reichler, T., and Roeckner, E.: Atmospheric component of the MPI-M Earth System Model: ECHAM6-HAM2, Journal of Advances in Modeling Earth Systems, 5, 146-172, 10.1002/jame.20015, 2013.

Stohl, A.: Characteristics of atmospheric transport into the Arctic troposphere. *J. Geophys. Res.* **111**, D11306, doi:10.1029/2005JD006888, 2006.

Stohl, A., Hittenberger, M., and Wotawa, G.: Validation of the Lagrangian particle dispersion model FLEXPART against large scale tracer experiments. Atmospheric Environment **32**, 4245-4264, 1998.

Stohl, A., Forster, C., Frank, A., Seibert, P., and Wotawa, G.: Technical note: The Lagrangian particle dispersion model FLEXPART version 6.2, Atmospheric Chemistry and Physics, 5, 2461-2474, 2005.

Stohl, A., Klimont, Z., Eckhardt, S., Kupiainen, K., Shevchenko, V. P., Kopeikin, V. M., and Novigatsky, A. N.: Black carbon in the Arctic: the underestimated role of gas flaring and residential combustion emissions, Atmospheric Chemistry and Physics, 13, 8833-8855, 10.5194/acp-13-8833-2013, 2013.

Stone, R. S., Herber, A., Vitale, V., Mazzola, M., Lupi, A., Schnell, R. C., Dutton, E. G., Liu, P. S. K., Li, S. M., Dethloff, K., Lampert, A., Ritter, C., Stock, M., Neuber, R., and Maturilli, M.: A three-dimensional characterization of Arctic aerosols from airborne Sun photometer observations: PAM-ARCMIP, April 2009, Journal of Geophysical Research-Atmospheres, 115, 10.1029/2009jd013605, 2010.

Sullivan, A. P., Peltier, R. E., Brock, C. A., de Gouw, J. A., Holloway, J. S., Warneke, C., Wollny, A. G., and Weber, R. J.: Airborne measurements of carbonaceous aerosol soluble in water over northeastern United States: Method development and an investigation into water-soluble organic carbon sources, Journal of Geophysical Research-Atmospheres, 111, 14, 10.1029/2006jd007072, 2006.

Tunved, P., Ström, J., and Krejci, R.: Arctic aerosol life cycle: linking aerosol size distributions observed between 2000 and 2010 with air mass transport and precipitation at Zeppelin station, Ny-Ålesund, Svalbard, Atmos. Chem. Phys., 13, 3643-3660, doi:10.5194/acp-13-3643-2013, 2013.

van der Werf, G. R., Randerson, J. T., Giglio, L., Collatz, G. J., Mu, M., Kasibhatla, P. S., Morton, D. C., DeFries, R. S., Jin, Y., and van Leeuwen, T. T.: Global fire emissions and the contribution of deforestation, savanna, forest, agricultural, and peat fires (1997–2009), Atmos. Chem. Phys., 10, 11707-11735, doi:10.5194/acp-10-11707-2010, 2010.

Vignati, E., M. Karl, M. Krol, J. C. Wilson, P. Stier and F. Cavalli, Sources of uncertainties in modelling black carbon at the global scale, Atmospheric Chemistry and Physics 10, 2595 – 2611, 2010.

von Salzen, K.: Piecewise log-normal approximation of size distributions for aerosol modelling, Atmospheric Chemistry and Physics, 6, 1351-1372, 2006.

von Salzen, K., Scinocca, J. F., McFarlane, N. A., Li, J. N., Cole, J. N. S., Plummer, D., Verseghy, D., Reader, M. C., Ma, X. Y., Lazare, M., and Solheim, L.: The Canadian Fourth Generation Atmospheric Global Climate Model (CanAM4). Part I: Representation of Physical Processes, Atmosphere-Ocean, 51, 104-125, 10.1080/07055900.2012.755610, 2013.

Wang, H., Easter, R. C., Rasch, P. J., Wang, M., Liu, X., Ghan, S. J., Qian, Y., Yoon, J. H., Ma, P. L., and Vinoj, V.: Sensitivity of remote aerosol distributions to representation of cloud-aerosol interactions in a global climate model, Geoscientific Model Development, 6, 765-782, 10.5194/gmd-6-765-2013, 2013.

Warneke, C., Froyd, K. D., Brioude, J., Bahreini, R., Brock, C. A., Cozic, J., de Gouw, J. A., Fahey, D. W., Ferrare, R., Holloway, J. S., Middlebrook, A. M., Miller, L., Montzka, S., Schwarz, J. P., Sodemann, H., Spackman, J. R., and Stohl, A.: An important contribution to springtime Arctic aerosol from biomass burning in Russia, Geophysical Research Letters, 37, 10.1029/2009gl041816, 2010.

Wang, Q., D. J. Jacob, J. R. Spackman, A. E. Perring, J. P. Schwarz, N. Moteki, E. A. Marais, C. Ge, J. Wang, and S. R. H. Barrett, Global budget and radiative forcing of black carbon aerosol: Constraints from pole-to-pole (HIPPO) observations across the Pacific, J. Geophys. Res. Atmos., 119, 195–206, doi:10.1002/2013JD020824, 2014.

Wofsy, S. C., Team, H. S., Cooperating Modellers, T., and Satellite, T.: HIAPER Pole-to-Pole Observations (HIPPO): fine-grained, global-scale measurements of climatically important atmospheric gases and aerosols, Philosophical Transactions of the Royal Society a-Mathematical Physical and Engineering Sciences, 369, 2073-2086, 10.1098/rsta.2010.0313, 2011.

Zaveri, R. A., and Peters, L. K.: A new lumped structure photochemical mechanism for large-scale applications, Journal of Geophysical Research-Atmospheres, 104, 30387-30415, 10.1029/1999jd900876, 1999.

Zaveri, R. A., Easter, R. C., Fast, J. D., and Peters, L. K.: Model for Simulating Aerosol Interactions and Chemistry (MOSAIC), Journal of Geophysical Research-Atmospheres, 113, 29, 10.1029/2007jd008782, 2008.

Zhang, K., O'Donnell, D., Kazil, J., Stier, P., Kinne, S., Lohmann, U., Ferrachat, S., Croft, B., Quaas, J., Wan, H., Rast, S., and Feichter, J.: The global aerosol-climate model ECHAM-HAM, version 2: sensitivity to improvements in process representations, Atmospheric Chemistry and Physics, 12, 8911-8949, 10.5194/acp-12-8911-2012, 2012.

Table 1. Model overview

Model Name	Model Type[1]	Horizontal/vertical resolution	Meteorological fields	Periods simulated / output temporal resolution	References
FLEXPART	LPDM	-	ECMWF Operational Analyses	2008-2009 3h	Stohl et al. (1998, 2005)
OsloCTM2	CTM	2.8°x2.8°, 60L	ECMWF Operational Analyses	2008-2009 3h	Myhre et al. (2009), Skeie et al. (2011a, 2011b)
NorESM	CCM	1.9°x2.5°, 26L	Internal, observed SST prescribed	2008-2009 3h	Kirkevåg et al. (2013), Bentsen et al. (2013)
TM4-ECPL	CTM	2°x3°, 34L	ECMWF ERA-interim	2008-2009 24h	Myriokefalitakis et al. (2011); Kanakidou et al. (2012); Daskalakis et al. (2014)
ECHAM6-HAM2	ACM	1.8°x1.8°, 31L	ECMWF Reanalysis	March-August, 2008, 1h	Stevens et al. (2013), Zhang et al. (2012)
SMHI-MATCH	CTM	0.57°x0.75°, 38L	ECMWF	2008, 2009 1h	Andersson et al. (2007), Robertson et al. (1999)
CanAM4.2	ACM	2.8°x2.8°, 49L	Nudged to ECMWF temp.and winds	2008-2009 3h	Von Salzen et al. (2013), von Salzen (2006)
DEHM	CTM	150km <60° N 50km >60°N, 29L	NCEP	2008-2009 3h	Christensen (1997), Brandt et al. (2012)
CESM1/CAM5.2	CCM	0.9°x1.25°, 30L	Internal, observed SST prescribed	2008-2009 1h	Liu et al. (2012), Wang et al. (2013)
WRF-Chem	CTM	0.75°x0.75°, 38L	Nudged to FNL	March-August 2008 3h	Grell et al. (2005), Zaveri et al. (1999), Zaveri et al. (2008)
HadGEM3	CCM	1.9°x1.3°, 63L	ECMWF ERA-interim	March-June, November 2008, January, May and November 2009 2h	Hewitt et al. (2011), Mann et al. (2010)

[1]Chemistry transport model (CTM), Lagrangian particle dispersion model (LPDM), chemistry climate model (CCM), aerosol chemistry model (ACM)

Table 2. Median observed eBC and modeled BC mass concentrations in ng/m^3 as well as measured and modeled sulfate (SO_4) concentrations in the Arctic during winter/spring (January to March) and summer (July to September). The data used are from the years 2008 and 2009 and were averaged for the three stations Alert, Barrow and Zeppelin for SO_4 and additionally for station Nord for BC. Notice that some models do not cover the whole periods completely (see Table 1).

Model/obs	Winter/Spring BC [ng/m^3]	Summer BC [ng/m^3]	Winter/Spring SO_4 [ng/m^3]	Summer SO_4 [ng/m^3]
Measured	46.5	3.8	561.0	103.2
Model mean:	20.1	6.1	331.6	136.9
FLEXPART	36.6	7.1		
OsloCTM2	8.0	1.2	81.6	98.3
NorESM	12.7	4.1	388.0	62.0
TM4	4.8	1.3	63.5	125.9
ECHAM6-HAM2	1.7	1.8	371.0	365.4
SMHI-MATCH	37.8	1.1	531.2	119.4
CanAM4.2	40.8	1.4	776.9	240.7
DEHM	55.6	11.6	422.2	56.1
CAM5.2	20.0	4.4	197.0	17.4
WRF-Chem	17.7	33.9	438.2	269.7
HadGEM3	1.6	0.6	46.4	13.8

Table 3: Slopes of regression lines between monthly mean concentrations of sulfate and (e)BC for the different stations. Slopes are calculated both for the observations and the model values. Values that are statistically significant at the 99.9% level are marked with an asterisk. For the mean over all sites/models, only the statistically significant values were averaged.

	Alert	Barrow	Pallas	Zeppelin	Mean
Observations	10.1*	6.4	8.4*	8.9*	9.1
Model mean	17.3	16.6	6.7	9.7	12.6
OsloCTM2	-8.6	2.4	-2.0	-5.5	-
NorESM	35.3*	27.8	0.4	12.1	35.3
TM4-ECPL	9.5	33.2*	5.8*	8.1	19.5
ECHAM6-HAM2	30.0	90.4	1.0	-746.4	-
SMHI-MATCH	25.6*	25.9*	0.4	10.9	25.7
CanAM4.2	18.2*	2.5	7.1	12.4*	15.3
DEHM	7.5*	5.7*	1.6*	6.7*	5.4
CESM1-CAM5	11.1*	8.9*	9.6*	9.9*	9.9
WRF-Chem	6.4*	9.3*	9.8*	2.4	8.5
HadGEM3	10.7	-8.7	-0.81	3.2	-

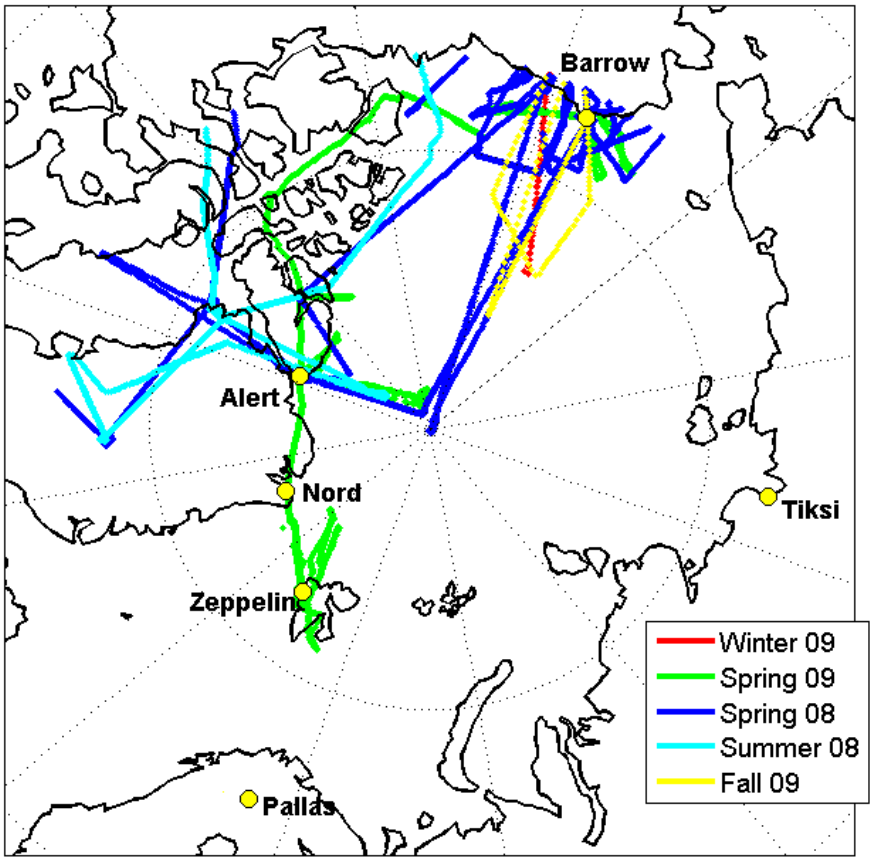

Figure 1. Map showing the locations of the measurement stations (yellow circles) and the flight tracks north of 70°N of all aircraft campaigns used in this study. Aircraft data were from the HIPPO (winter 2009 and fall 2009), ARCTAS (spring and summer 2008), ARCPAC (spring 2008) and PAMARCMiP (spring 2009) campaigns.

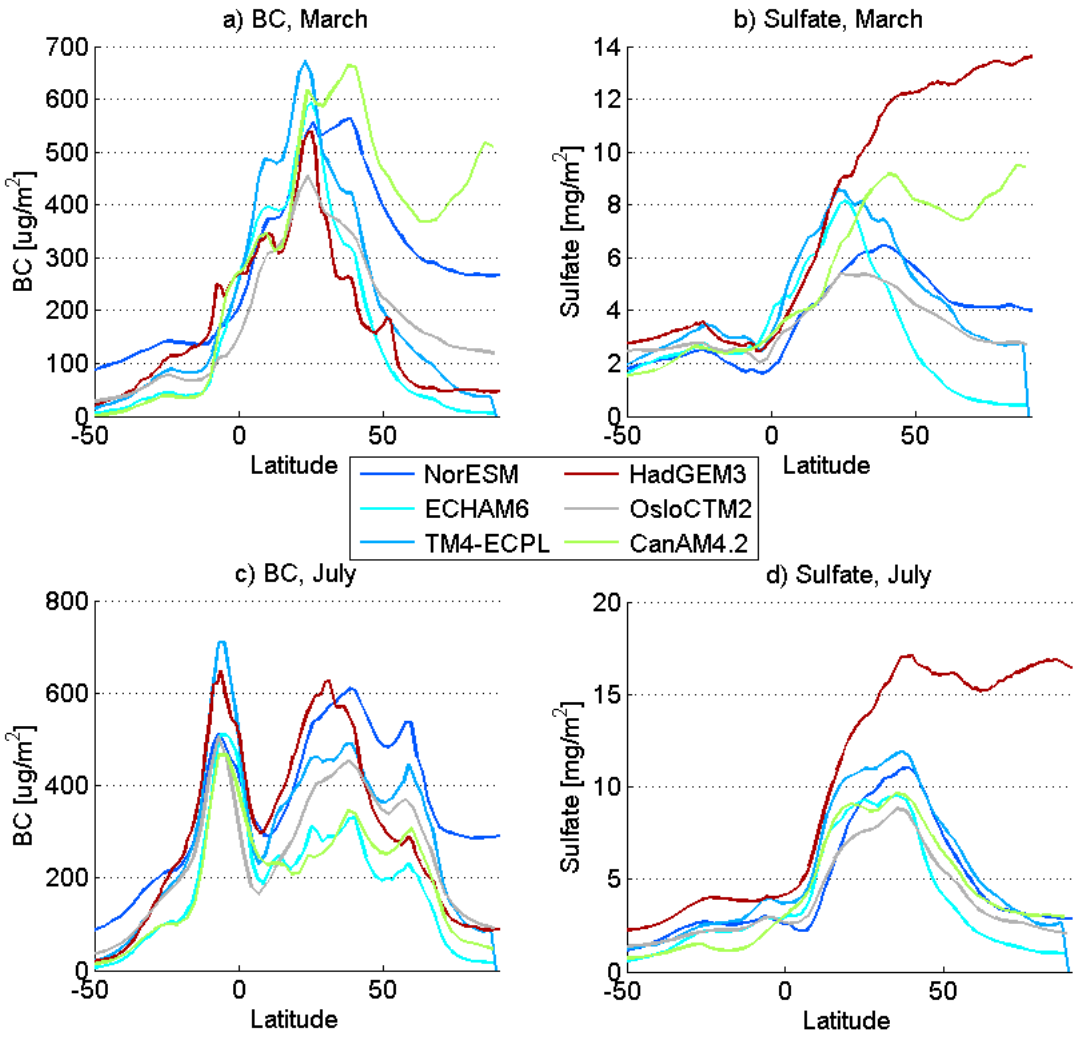

Figure 2: BC (a, c) and sulfate (b, d) column mass loadings averaged over all longitudes as a function of latitude (for the range 50°S to 90°N) for March (a-b) and July (c-d).

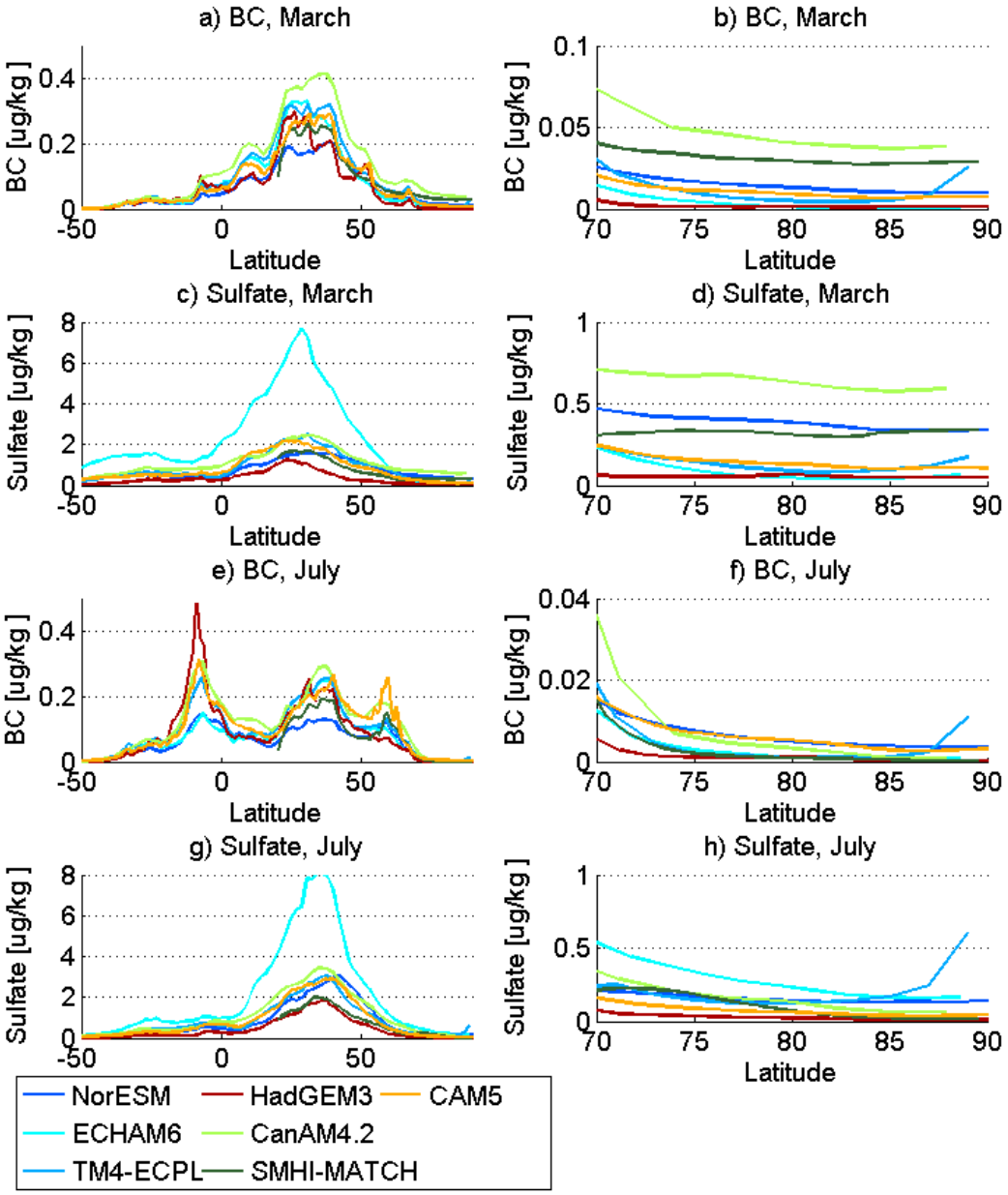

Figure 3: BBC (a-b, e-f) and sulfate (c-d, g-h) mass mixing ratios at the surface averaged over all longitudes as a function of latitude (for the range 50°S to 90°N) for March (a-d) and July (e-h). The right panels show the same data as the left panels, but only for 70-90°N and with an adjusted ordinate scale.

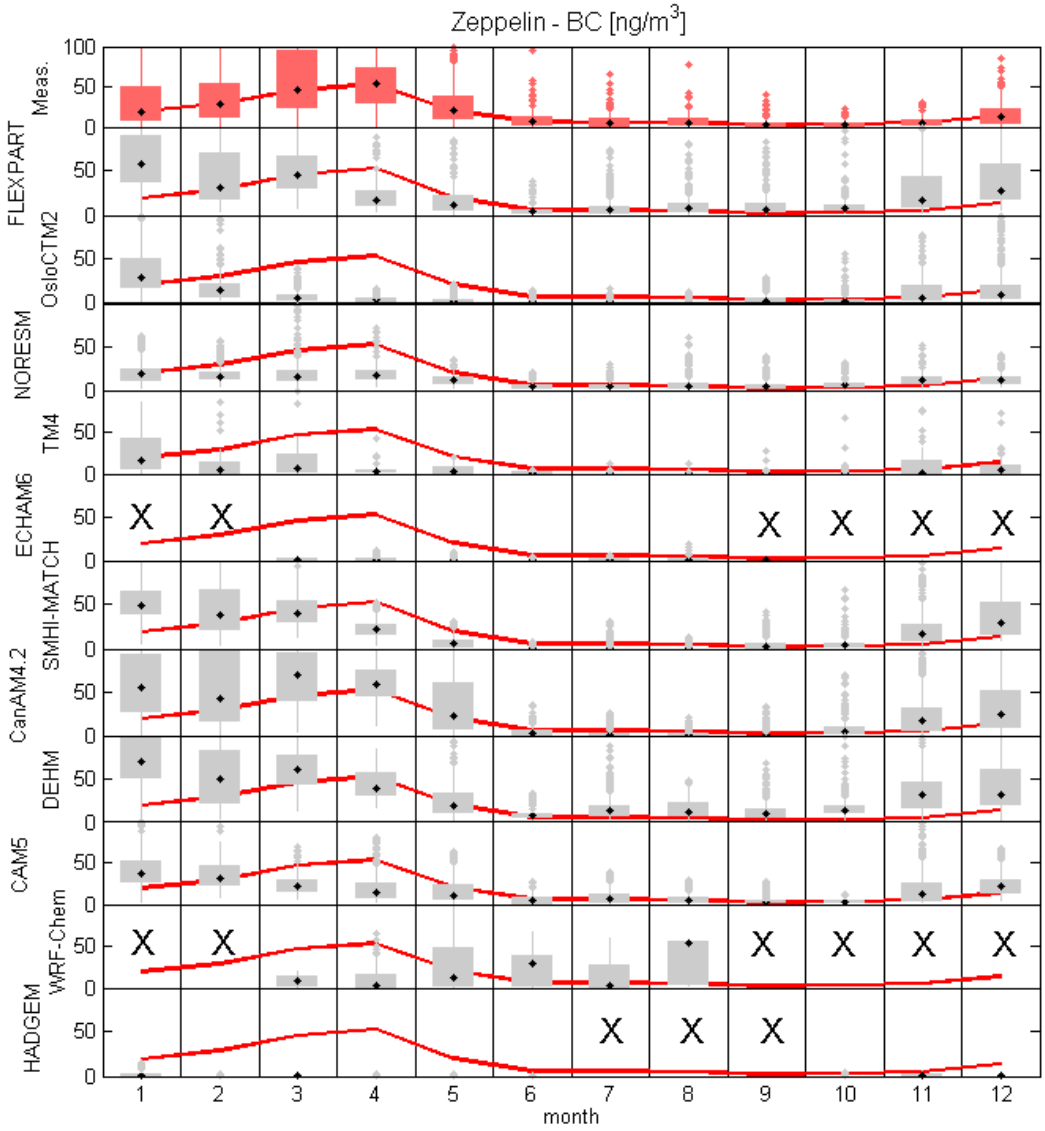

Figure 4. Observed and simulated mean annual cycle of (equivalent) BC mass concentrations [ng/m^3] at the Zeppelin station, shown as monthly frequency distributions using data from the years 2008 and 2009. The uppermost panel shows monthly frequency distributions of the observed eBC concentrations, the other panels show monthly frequency distributions of the modeled BC concentrations. Black dots depict the monthly median value, the grey boxes span the range between the 25th and 75th percentiles. The red line connects the monthly medians of the observed eBC concentrations in the uppermost panel and is repeated in all other panels for the convenience of comparing modeled and measured values. Missing model data are denoted with "X". Notice that some models have very low BC mass concentrations, which are difficult to see on the scale used.

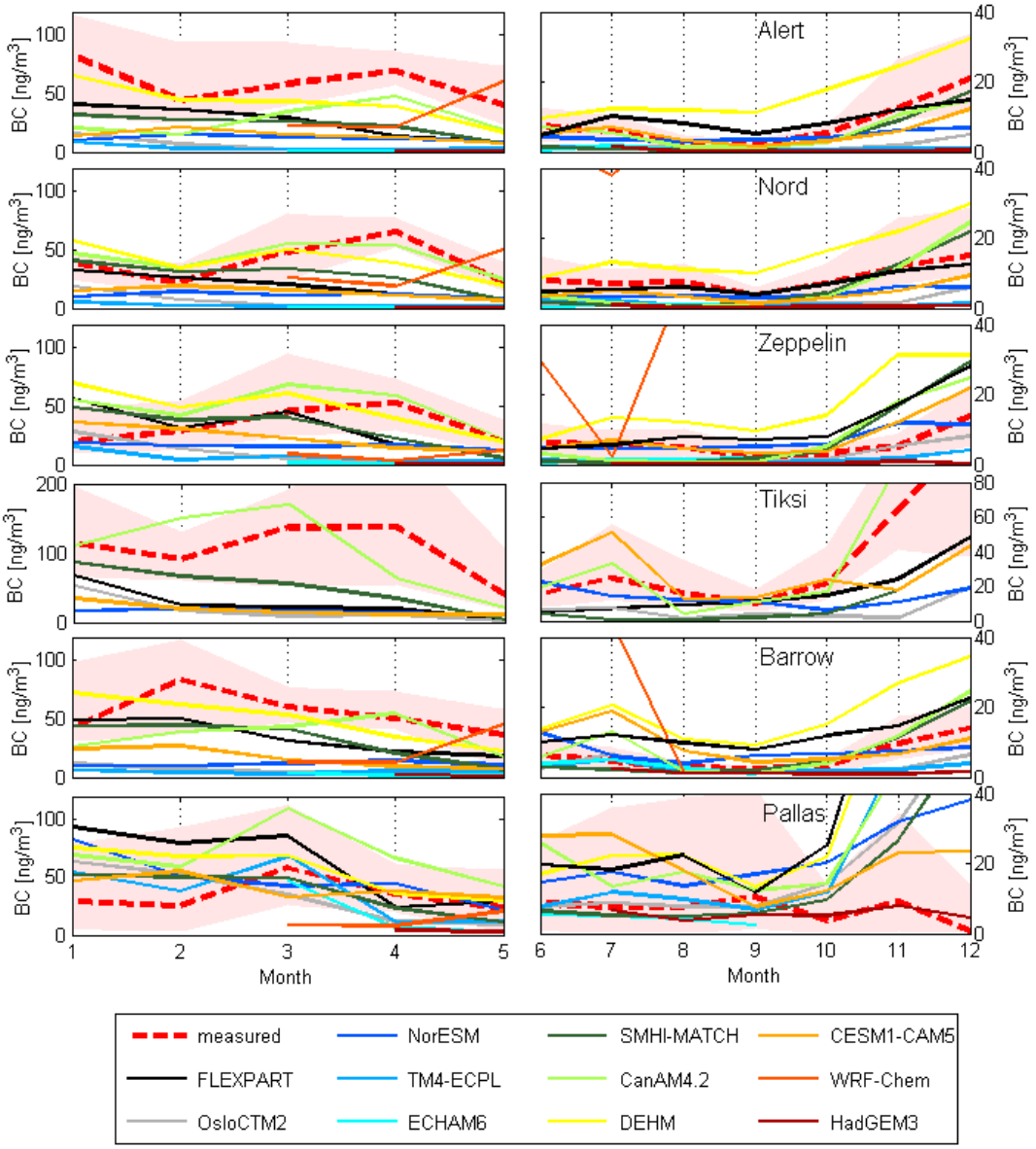

Figure 5. Monthly (month is displayed on the abscissa) median observed eBC and modeled BC concentrations for the six stations for late winter/spring (left column) and summer/fall (right column). The red dashed lines connect the observed median values, the light red shaded areas span from the 25th to the 75th percentile of the observations. Modeled median values are shown with different lines according to the legend. Notice the difference in concentration scales used for the left and right panels and also for the Tiksi station.

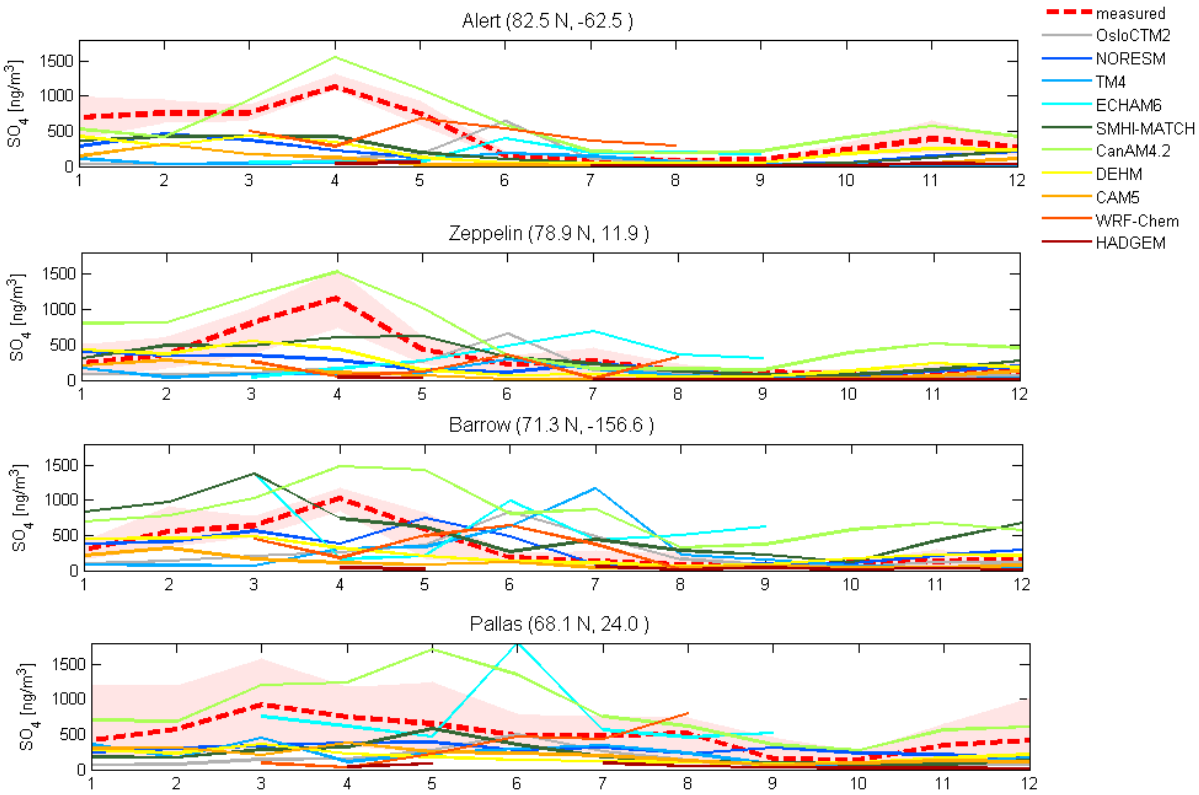

Figure 6. Monthly (month is displayed on the abscissa) median observed and modeled sulfate concentrations for the four stations. The red dashed lines connect the observed median values, the light red shaded areas span from the 25th to the 75th percentile of the observations. Modeled median values are shown with different lines according to the legend.

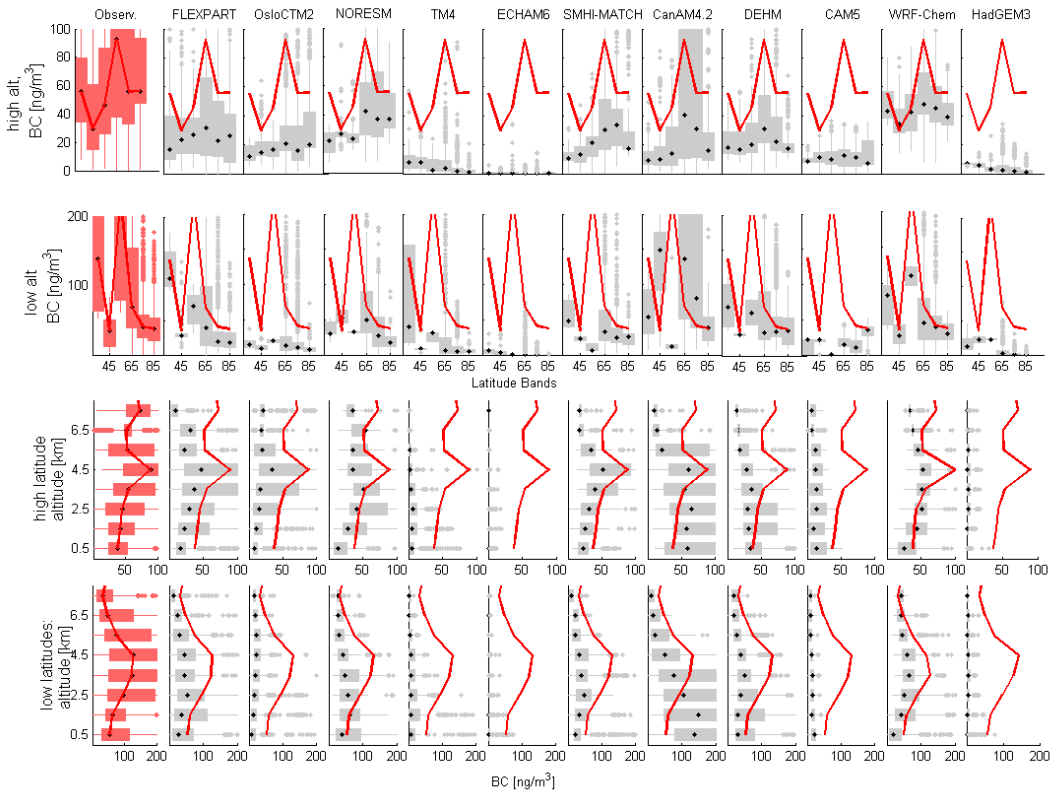

Figure 7: Comparison of modeled BC with observed rBC mass concentrations from the ARCTAS-spring and ARCPAC campaigns in spring 2008. The leftmost column shows box and whisker plots of observed rBC concentrations in ng/m^3. The black dots as well as the red lines represent the median values. The other columns show the modeled BC concentrations for FLEXPART, OsloCTM2, NorESM, TM4, ECHAM6-HAM2, SMHI-MATCH, CanAM4.2, DEHM, CAM5, WRF-Chem and HadGEM3. The top (second from top) row represents median (r)BC concentrations for altitudes below (above) 3 km asl as a function of latitude by binning the data into 10° latitude bands. The third (bottom) row shows median (r)BC concentrations for latitudes north of (south of) 70^{0}N as a function of altitude by binning the data into 1-km height intervals.

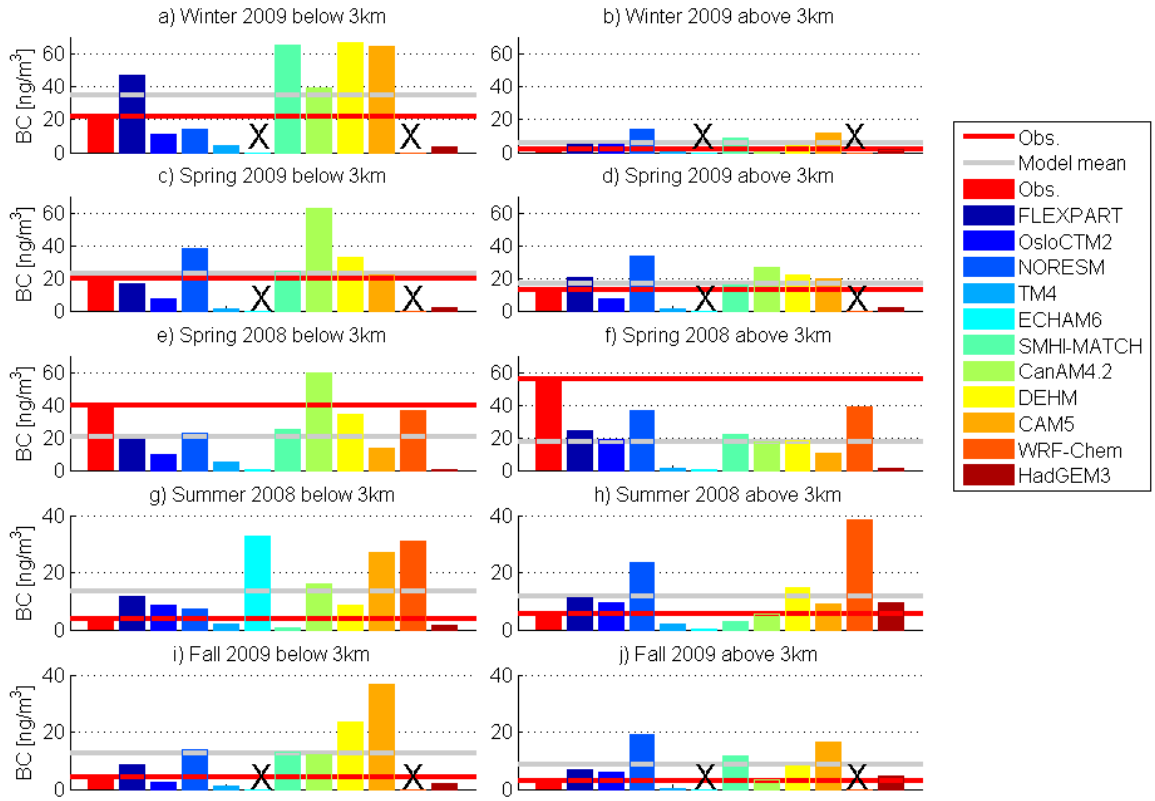

Figure 8: Median observed rBC and modeled BC mass concentrations for the winter 2009 HIPPO (a, b) spring 2009 PAMARCMiP (c-d) spring 2008 ARCTAS/ARCPAC (e- f), summer 2008 ARCTAS (g-h) and the fall 2009 HIPPO (i-j) aircraft campaigns. The red bar and the red line show the observations, the colored bars the various models, the grey line shows the mean value of all model medians. Results are shown separately for measurements below 3 km (left row) and above 3 km (right row). Notice that the concentration scales on the ordinates are different for the individual panels.

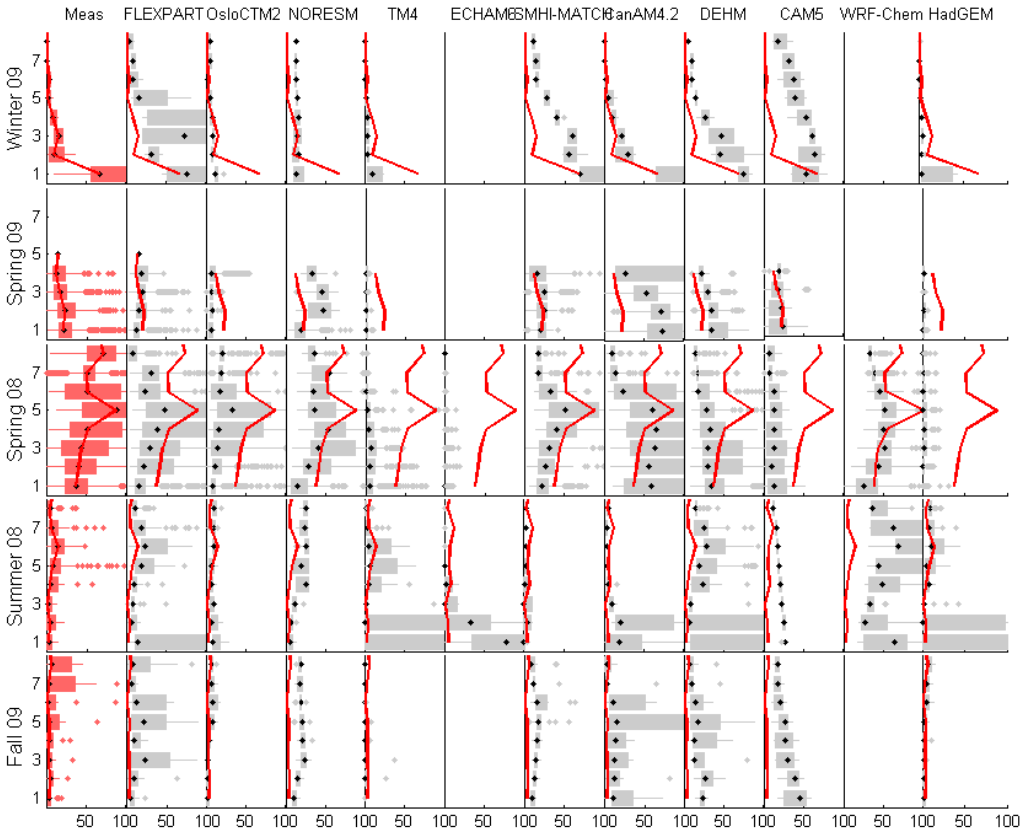

Figure 9: Comparison of modeled BC with observed rBC mass concentrations as a function of altitude for all data taken north of 70°N, for the different campaigns. The leftmost column shows box and whisker plots of observed rBC concentrations in ng/m^3. The black dots as well as the red lines represent the median values. The other columns show the modeled BC concentrations for FLEXPART, OsloCTM2, NorESM, TM4, ECHAM6-HAM2, SMHI-MATCH, CanAM4.2, DEHM, CAM5, WRF-Chem and HadGEM3.

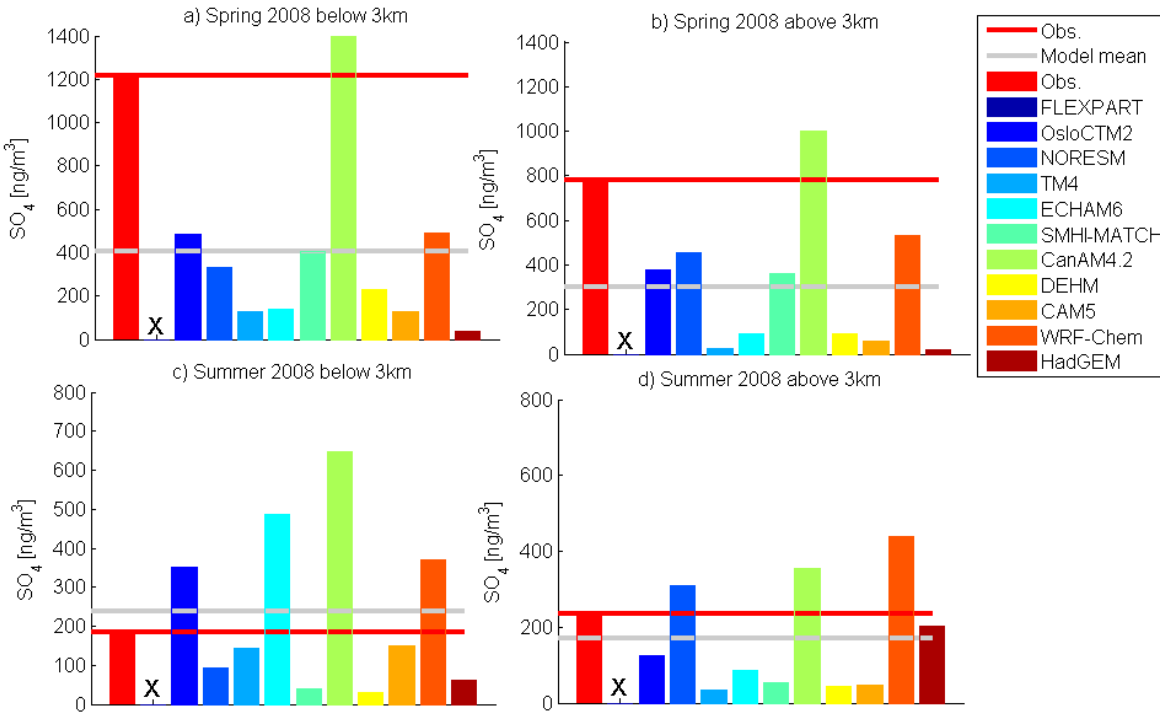

Figure 10: Median SO_4 concentration for the ARCTAS/ARCPAC spring 2008 (a, b) and ARCTAS summer 2008 (c, d) campaigns. The red bar and the red line shows the observations, the colored bars the various models. The analysis is performed for measurements below 3 km (left row) and above 3 km (right row). Note: each row has a different y-axis.

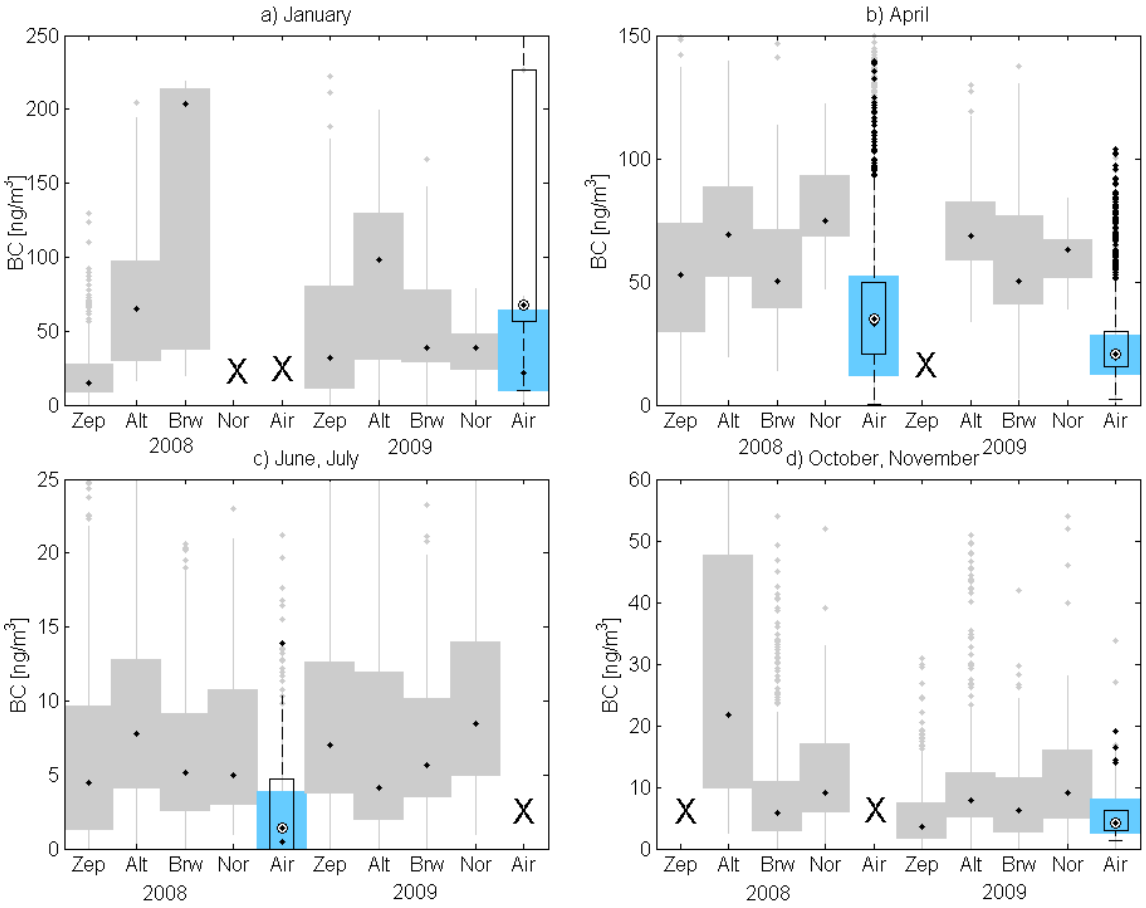

Figure 11: Comparison of eBC [ng/m^3] measured at the stations Zeppelin (Zep), Alert (Alt), Barrow (Brw) and Station Nord (Nor) (grey bars) and rBC [ng/m^3] measured by aircraft (Air) in the lowest 3 km and 1 km, north of 70°N (blue bars) for the years 2008 and 2009 for a) January, b) April, c) June and July and d) October and November. The black dots represent the median, and the boxes the interquartile range. For the aircraft measurements, the blue boxes show the results for the lowest 3 km, the black box outlines show the results for the lowest 1 km.

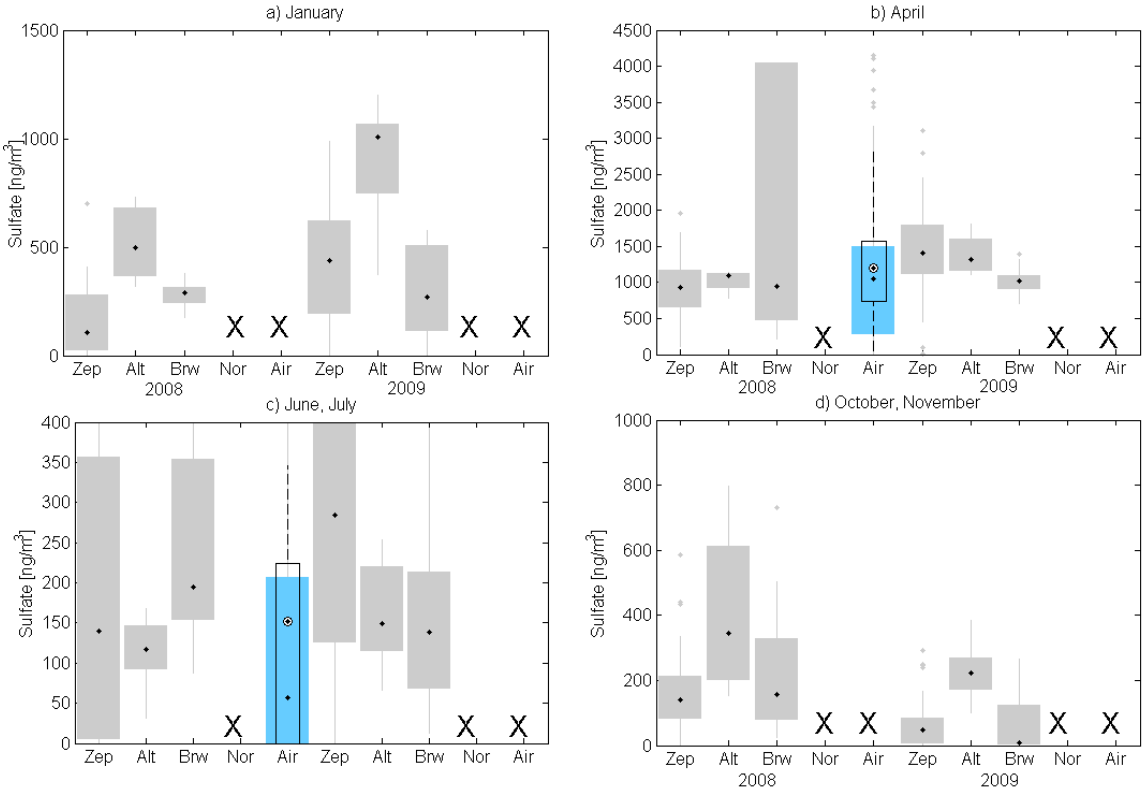

Figure 12: Same as figure 9, but for sulfate.

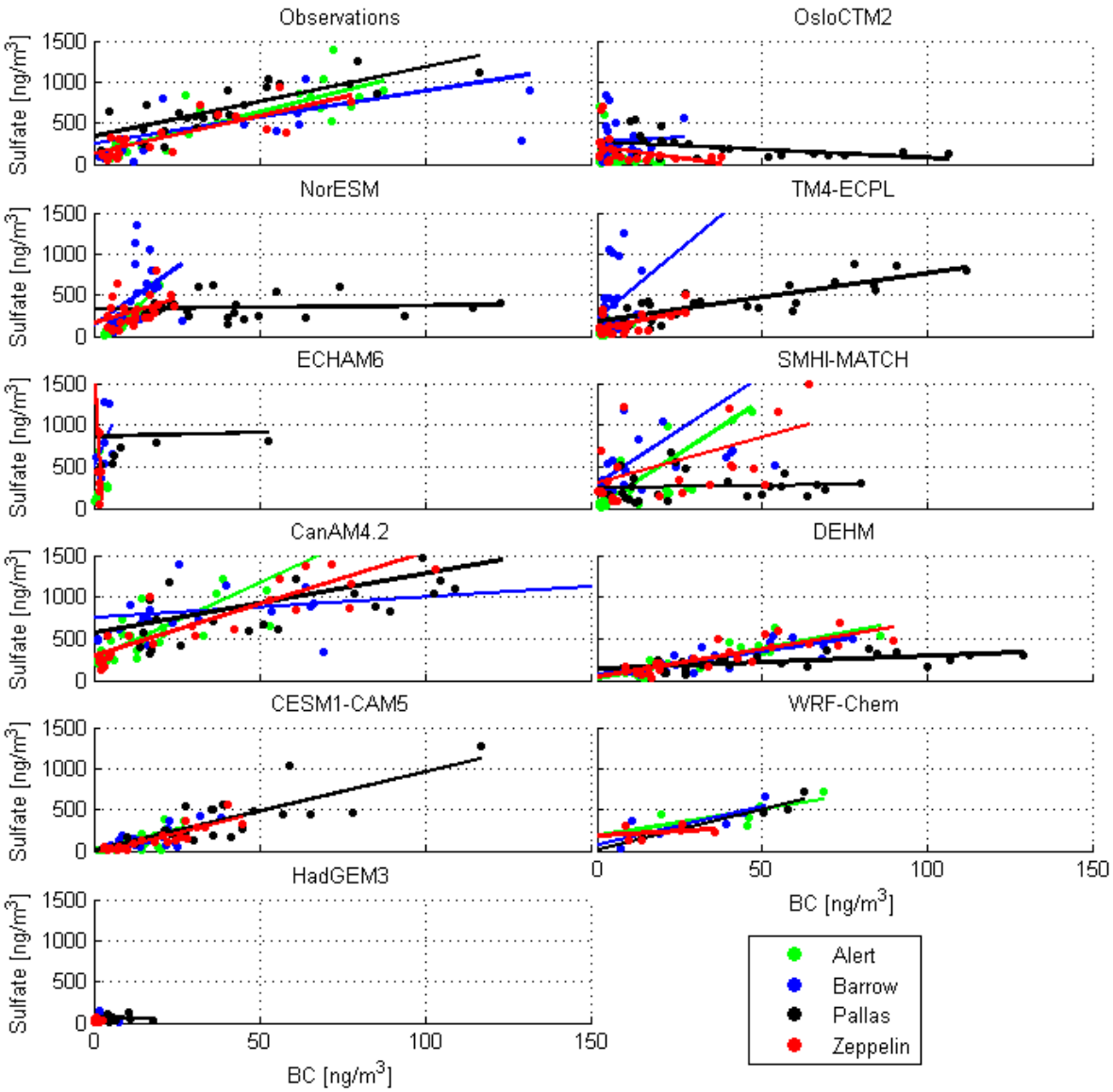

Figure 13: Correlation plots of monthly mean sulfate and eBC concentrations for the observations (top left) and the different models sampled at the observation sites.